Soil Dynamics and Earthquake Engineering 104 (2018) 15–32

Contents lists available at ScienceDirect

Soil Dynamics and Earthquake Engineering

journal homepage: www.elsevier.com/locate/soildyn

Seismic behavior of irregular reinforced-concrete structures under multiple earthquake excitations

Resat Oyguc[a,*], Cagatay Toros[a], Adel E. Abdelnaby[b]

[a] Istanbul Technical University, Institute of Earthquake Engineering and Disaster Management, Maslak 34469, Istanbul, Turkey
[b] Department of Civil Engineering, The University of Memphis, 106C Engineering Science Building, 3815 Central Avenue, Memphis, TN 38152, United States

ARTICLE INFO

Keywords:
Multiple earthquake
Irregular RC structures
Degrading material models
Nonlinear time history analysis
N2 method
Extended N2 method
Residual displacements
Aftershocks

ABSTRACT

Reconnaissance studies on the recent Tohoku earthquake have reported collapse of structures due to multiple earthquake excitations in the earthquake-affected region. Strength and stiffness degradation is shown to be the primary reason for the observed damage. The present study aims to investigate the degrading behavior of irregularly built reinforced concrete structures subjected to the Tohoku ground motion sequences. Three-dimensional numerical models of three irregular reinforced concrete structures are developed. The structural characteristics of these buildings are then altered to achieve a regular case. The models contain appropriate damage features that can capture both the irregularity and material deterioration effects. The capacities of both cases are evaluated using the N2 and extended N2 procedures. The degrading models are then used for ground motion sequences measured at 23 selected stations. The results indicate that multiple earthquake effects are significant, and irregularity effects increase the dispersed damage under these excitation sequences.

1. Introduction

Reinforced concrete (RC) structures during the recent Tohoku and Christchurch earthquakes experienced excessive loss of stiffness and strength due to repeated shaking. Many RC buildings that were not heavily damaged immediately after the main excitations have collapsed because of aftershocks. Correspondingly, many previous in situ examinations have reported the unfavorable effects of multiple ground excitations on structural systems.

In literature, to determine the response of structures by modeling their structural behavior, single-degree-of-freedom (SDOF) systems were extensively used because of their simplicity. Degrading systems were first introduced by Aschheim and Black [1], who used a modified Takeda hysteretic model. Their model was able to capture both the pinching and strength degradation effects. Base on their conclusions, the displacement response of an initially damaged SDOF system was approximately the same as that of its undamaged counterpart after the peak displacement was reached. Amadio et al. [2] investigated the nonlinear behavior of SDOF structures under multiple excitations using three different hysteretic models: *non-degrading stiffness and strength, degrading stiffness and non-degrading strength, degrading stiffness and strength*. They concluded that elastoplastic systems can be classified as the most vulnerable SDOF systems. Hatzigeorgiou and Beskos [3] conducted an extensive parametric study to obtain an appropriate inelastic displacement ratio while examining the period of vibration, viscous damping ratio, strain-hardening ratio, force reduction factor and soil class. They revealed that the repeated earthquakes have significant effect on both the inelastic displacement ratios and maximum inelastic displacement values of SDOF systems.

In order to consider degrading behavior of moment resisting frame systems in structural analyses, component-level-based degrading models (multi-degree-of-freedom systems) have been developed and widely used in the literature. These models utilize nonlinear moment-rotation relationships at locations of possible plastic hinges (beam and column ends) that consider both stiffness and strength degradation. The idealization of assuming concentrated inelasticity at predefined plastic hinge locations lacks the consideration of localized failure modes and therefore can lead to inaccurate assessment of degrading response under earthquake sequences. Hatzigeorgiou and Liolios [4] investigated the effectiveness of component-level-based models under multiple excitations, assuming bilinear moment–rotation relationships at beam–-column connections. Moreover, beam and column elements are assumed to behave elastically. These developed models can also consider second-order effects; however, they exclude material deterioration effects. The mentioned studies highlighted the fact that residual displacements play a major role on stiffness degradation.

To the best of the authors' knowledge, Abdelnaby and Elnashai [5] are the only researchers who have studied the effects of multiple

* Corresponding author.
E-mail address: oyguc@itu.edu.tr (R. Oyguc).

http://dx.doi.org/10.1016/j.soildyn.2017.10.002
Received 19 February 2017; Received in revised form 15 June 2017; Accepted 1 October 2017

earthquakes using distributed plasticity models, including the material deterioration effects on two-dimensional (2-D) structures. They utilized nonlinear dynamic analyses to incorporate structural damage features in their models. They investigated the degradation behavior of RC structures under the Tohoku and Christchurch earthquake sequences. They concluded that neither system-level-based models nor component-level-based models can accurately estimate the degradation response.

This study is unique because it considers the effects of multiple earthquake excitations for irregular structures. Furthermore, a plastic-damage model of concrete developed by Lee and Fenves [6], and the modified Menegotto-Pinto steel model [7,8] that are previously utilized and implemented by Abdelnaby and Elnashai [5] to ZEUS-NL [9] are used to evaluate the seismic response of irregularly build RC structures. The reader is referred to the cited reference for more information regarding the material model. The aim of this study is to evaluate the seismic performance of irregularly designed RC buildings when subjected to strong ground motion sequences. To properly assess the seismic response of three previously selected RC buildings, 516 nonlinear dynamic analyses are executed using ZEUS-NL [9], considering the Tohoku earthquake sequence. The structures are analyzed for two cases: (1) in their original form and (2) after modifying the geometry with the objective of reducing their level of irregularity without altering the overall stiffness. The results are then discussed in terms of comparing the degrading and non-degrading models subjected to this multiple earthquake sequence. Furthermore, the plastic hinge distributions, residual displacements, and interstory drift ratios are evaluated by applying the aforementioned material level-based model.

2. Earthquake ground motion sequences

A devastating earthquake with a moment magnitude (M_w) of 9.0 occurred at 14:46 (JST GMT + 9) on March 11, 2011, in Japan. This high-M_w earthquake is categorized among the most powerful excitations in the world since the 1900s, when modern record keeping began [10]. The Japan Meteorological Agency (JMA) [11] reported that the focal mechanism of this earthquake excitation was a reverse fault with a compression axis in the east-to-west direction at a depth of 24 km. The earthquake occurred at the plate boundary between the North American and Pacific plates [12].

It should be noted that this earthquake is unique because of its foreshocks and aftershocks. Zhao [13] highlighted that the earthquake sequence started with a 7.3-magnitude foreshock two days before the mainshock, which triggered vigorous aftershocks. Kazama and Noda [14] reported 593 aftershocks in a 3-month period between March 11 and June 11, of which five had magnitudes of 7.0 or greater. Certainly, the Tohoku excitation, with a magnitude of 9.0, greatly increased the seismic activity in the broad regions in and around the Japanese archipelago. More than 10,000 aftershocks with magnitudes of at least 3.0 occurred in the forearc area [15]. The epicenter of the aforementioned ground excitation, the foreshock, and the aftershocks with magnitudes greater than 7.0 are marked on the map in Fig. 1.

In this study, 23 stations that recorded the strong ground motions are considered. The locations and maximum peak ground acceleration (PGA) values of these stations are illustrated in Fig. 1. Records were acquired from the National Research Institute for Earth Science and Disaster Prevention (NIED) [16] data bank. The reader is referred to the cited document for more information regarding the strong ground motion parameters. The distances from the considered stations to the epicenter, soil properties upon which the stations are built, and PGA values are the key parameters for selecting the records. Additionally, to overcome the near fault effects, only records of stations that are at least 20 km away from the epicenter have been considered. Furthermore, liquefaction effects are neglected. Hence, records having shear wave velocities for the top 30 m of the subsurface profile ($V_{s,30}$) in the range of 360–800 m/s are used in the nonlinear dynamic analyses. For brevity, the authors decided to consider the earthquake ground motion sequences having PGA values between 0.20 g and 0.80 g. Values exceeding 0.80 g are omitted owing to their destructiveness. Therefore, 43 ground motion sequences have been selected for use in the conducted nonlinear dynamic analyses. The vertical effects of the earthquake sequences have been neglected in accordance with FEMA 356 [17].

The spectral displacement (S_d), spectral acceleration (S_a), pseudo spectral velocity (PS_v), and pseudo spectral acceleration (PS_a) graphs of the sequences that are used in this study are plotted in Fig. 2. Additionally, plots of the mean, mean + standard deviation and mean – standard deviation are presented in Fig. 2. For comparison, the response spectrum for soil type B of Eurocode 8 (EC8) [18] is plotted in the same figure. It can be inferred from the figure that the mean response spectra of the selected earthquake ground motions are in accordance with that of EC8 [18] for low period.

3. Description of case-study buildings

In this study, three plan-asymmetric RC buildings are considered: Seismic Performance Assessment and Rehabilitation of Existing Buildings (SPEAR), Innovative Concepts for Seismic Design of New and Existing Structures (ICONS), and a school building in Van, Turkey. The SPEAR and ICONS frames were a part of an extensive experimental investigation research program funded by the European Union (EU). Both buildings have been designed and built to represent RC structures with no seismic detailing. The school building was designed in accordance with Turkish Earthquake Code (TEC) [19]. It should be strongly emphasized that the majority of existing RC buildings in Turkey are similar to that studied herein. Further details regarding the selected irregular buildings are given in the following sections. Moreover, to consider the seismic response of irregular RC buildings under multiple earthquake excitations, the selected structures are analyzed for two cases. In the first case, they are analyzed as designed; in the second case, the geometry is modified without altering the overall stiffness of the structures.

3.1. SPEAR building for as designed and modified cases

The SPEAR building was built for performing pseudo-dynamic tests in the European Laboratory for Structural Assessment (ELSA) in Ispra, Italy. The structure was designed by Fardis [20] according to the construction practice and materials used in Greece in the early 1970s. The building was built irregularly in plan, but it was regular in elevation. It had three stories, and the story heights were 3 m. It has two bays in the horizontal (X) and transverse (Y) directions. The structure was tested in 2004 using a full-scale pseudo-dynamic test [21]. The plan layout, elevation and the reinforcement detailing of the building are shown in Fig. 3. As highlighted in this paper, the single column (C6) with a cross section of 25 cm × 75 cm makes the structure stiffer and stronger along the Y-direction.

The compressive strength of concrete [22] and yield strength of steel [23] are selected as 25 MPa and 400 MPa, respectively. The calculated torsional characteristics according to EC8 [18] are presented in Table 1, where e_{ox} and e_{oy} are the eccentricities measured along the X- and Y-directions, respectively, r_x and r_y are the torsional radii measured along the X- and Y-directions, respectively, and l_s is the radius of gyration of a floor in plan. More details regarding the structural properties of the building can be found in the studies by Stratan and Fajfar [24] and Papanikolau et al. [23].

Owing to the large eccentricities in the Y-direction, it was decided that the structure be remodeled and the regular case be performed in this direction. In order to not alter the rigidity of the structure and retain the same stiffness value, the dimensions of the columns circled in Fig. 4(i.e. C6, C7, and C8) are altered. Consequently, the stiffness values of the structure in the Y-direction are calculated as approximately 152 kN/m and 149 kN/m, before and after remodeling the building, respectively. Furthermore, the lateral stiffness difference ratio of the

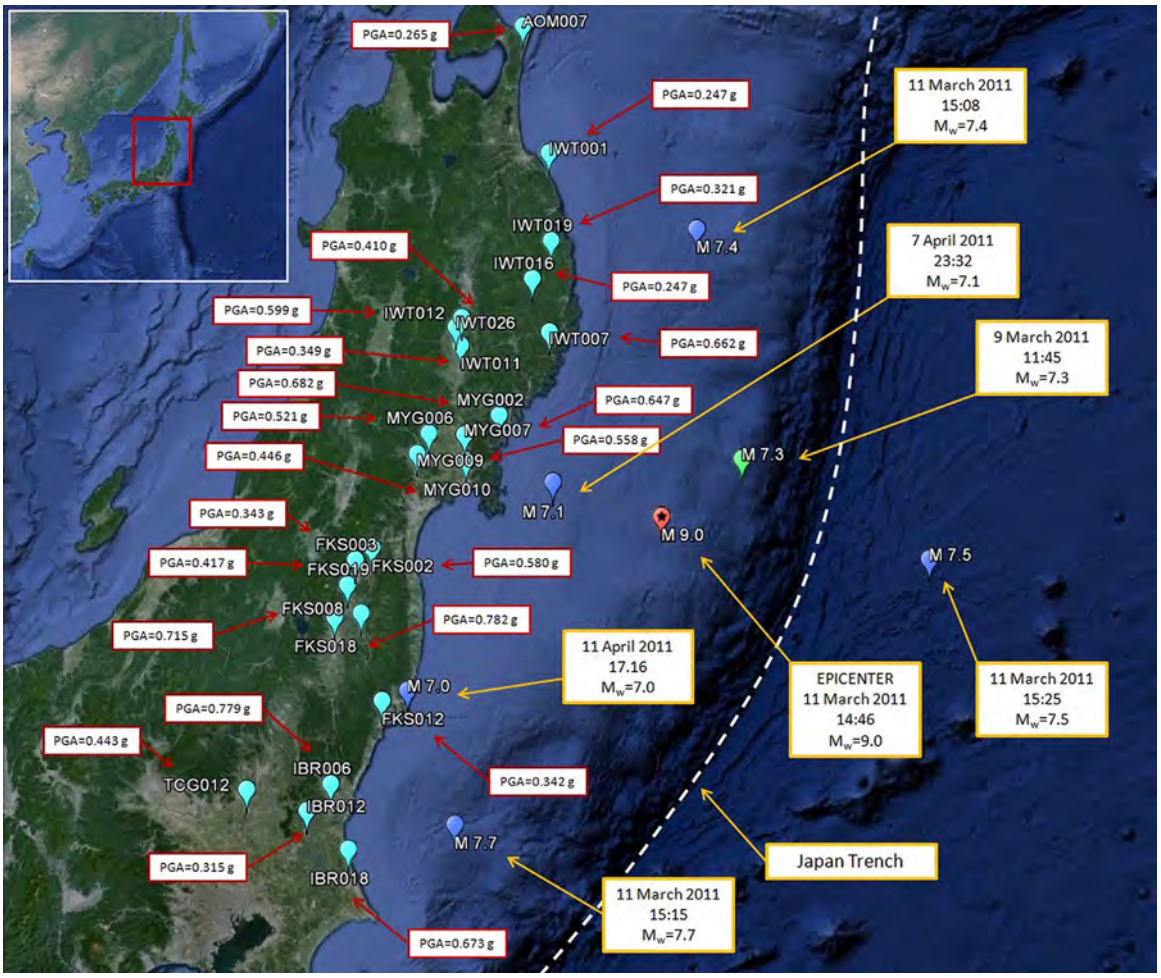

Fig. 1. Epicenter locations of the mainshock and aftershocks for the considered stations with recorded peak ground acceleration values.

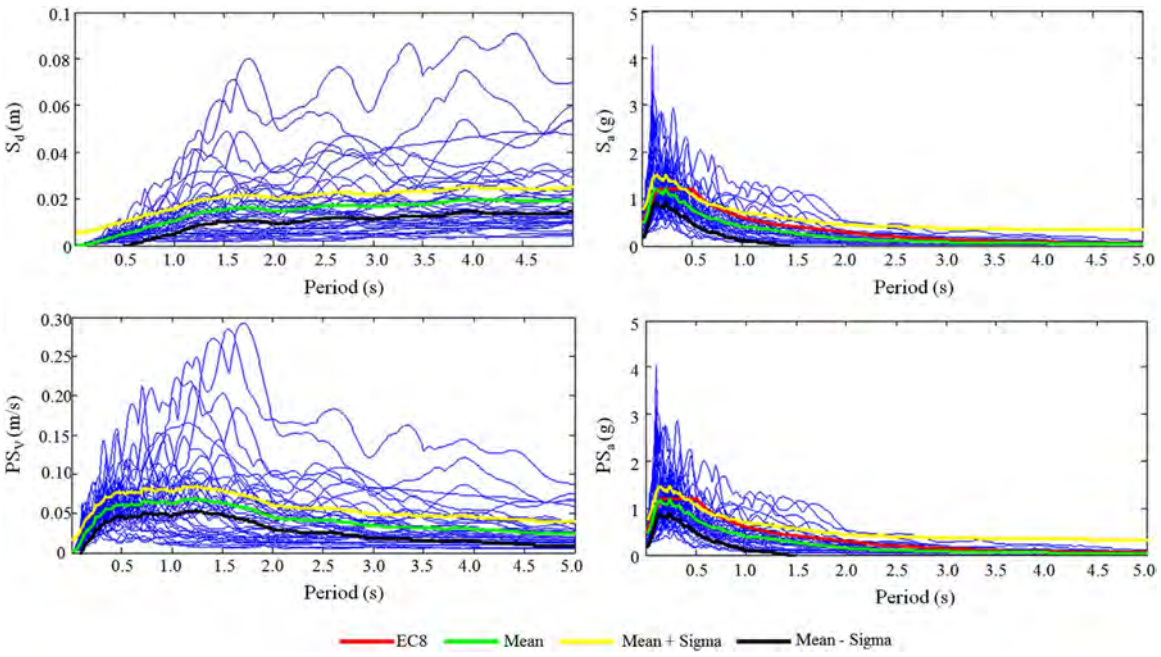

Fig. 2. Strong ground motion parameters and response spectra.

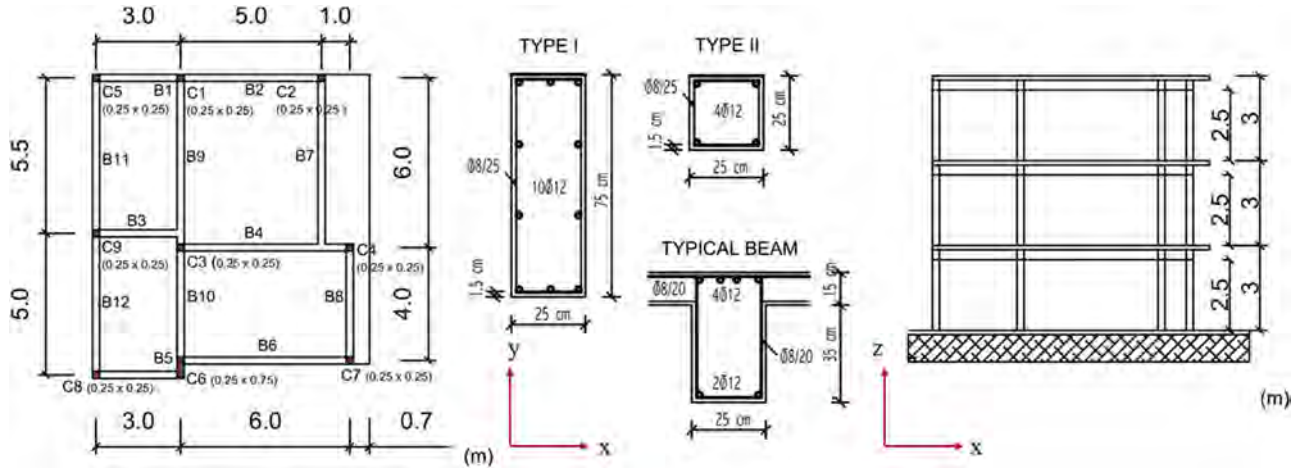

Fig. 3. General layout of the SPEAR building: plan (left), height configuration (right).

Table 1
Calculated irregularity parameters for SPEAR building.

e_{ox} (m)	r_x (m)	$0.3r_x$ (m)	e_{oy} (m)	r_y (m)	$0.3r_y$ (m)	l_s (m)
1.31	1.45	0.435	1.04	3.53	1.06	4.38

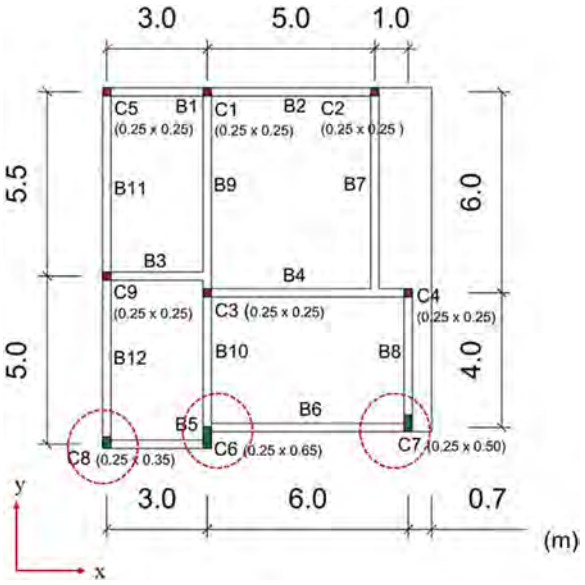

Fig. 4. Plan layout of remodeled SPEAR building.

Table 2
Irregularity parameters after modifying selected structural elements for SPEAR building.

e_{ox} (m)	r_x (m)	$0.3r_x$ (m)	e_{oy} (m)	r_y (m)	$0.3r_y$ (m)	l_s (m)
0.23	1.86	0.558	1.36	5.86	1.76	4.38

regular to the irregular case is calculated as 2%. The corresponding irregularity parameters of the modified buildings for the considered direction are provided in Table 2.

3.2. ICONS frame for as designed and modified cases

The ICONS frame was also built for the performance of pseudo-dynamic tests in ELSA. Two separate frames were constructed for this experimental program: one was constructed with infill panels and the other was bare [25]. In this present work, only the bare frame is considered. The structure is a four-story building designed by Carvalho et al. [26] for gravity loads, and it was built to represent typical 1960s RC structures with no seismic detailing. The story heights are 2.7 m, and the structure has three bays in the horizontal direction. Fig. 5 shows the plan layout and reinforcement detailing of the building. The ICONS frame is considered to be a regular structure. The compressive strength of concrete and yield strength of steel are given as 16.3 MPa and 343 MPa, respectively [25]. In this study, the ICONS frame is remodeled for the irregular case by applying the criteria related to setbacks in EC8 [18] for irregularity in elevation. For clarity, the remodeled case is presented in Fig. 6. The dashed part in figure was removed from the original structure in order to create setbacks.

3.3. RC school building for as designed and modified cases

This structure was constructed in the Van Province, which is in the eastern part of Turkey. Two earthquakes struck the region on October 23 and November 9 of 2011, with M_w of 7.2 and 5.6, respectively. The reader is referred to [27–29], and [30] for more details regarding the aforementioned strong ground motions. After reconnaissance studies, the considered RC school building had been reported as heavily damaged. Even though schools are classified as buildings that have to be used immediately after an earthquake in TEC [31], most of the school buildings that were constructed in the earthquake-affected region may be classified as non-engineered structures. It was observed that most of the structures do not obey the rules that have been laid down in the latest design codes [30].

The damaged RC school building has three stories. The height of the basement floor is 3.5 m and, it is surrounded by concrete shear walls; in contrast, the upper floors are 3 m in height. Hence, the structure can be considered as irregular in elevation, but regular in plan. Fig. 7 shows the plan layout and reinforcement detailing of the building. To determine the concrete strength, concrete core samples were taken in accordance with the procedures described in TEC [31]. The characteristic cylinder compressive strength of building was found to be 20 MPa. Moreover, the steel grade used in the RC school building is classified as STIII, which has a characteristic yield strength of 420 MPa and an estimated elastic modulus of 210 GPa.

Irregularity check results were obtained according to TEC [31]. In this code, η_{bi} is the torsional irregularity factor, which is defined for any of the two orthogonal earthquake directions as the ratio of the maximum relative story drift at any story to the average relative story drift at the same story in the same direction. This ratio should be less than 1.2 to classify a building as regular. For the present case, this value has been calculated as 1.06, which indicates regular behavior.

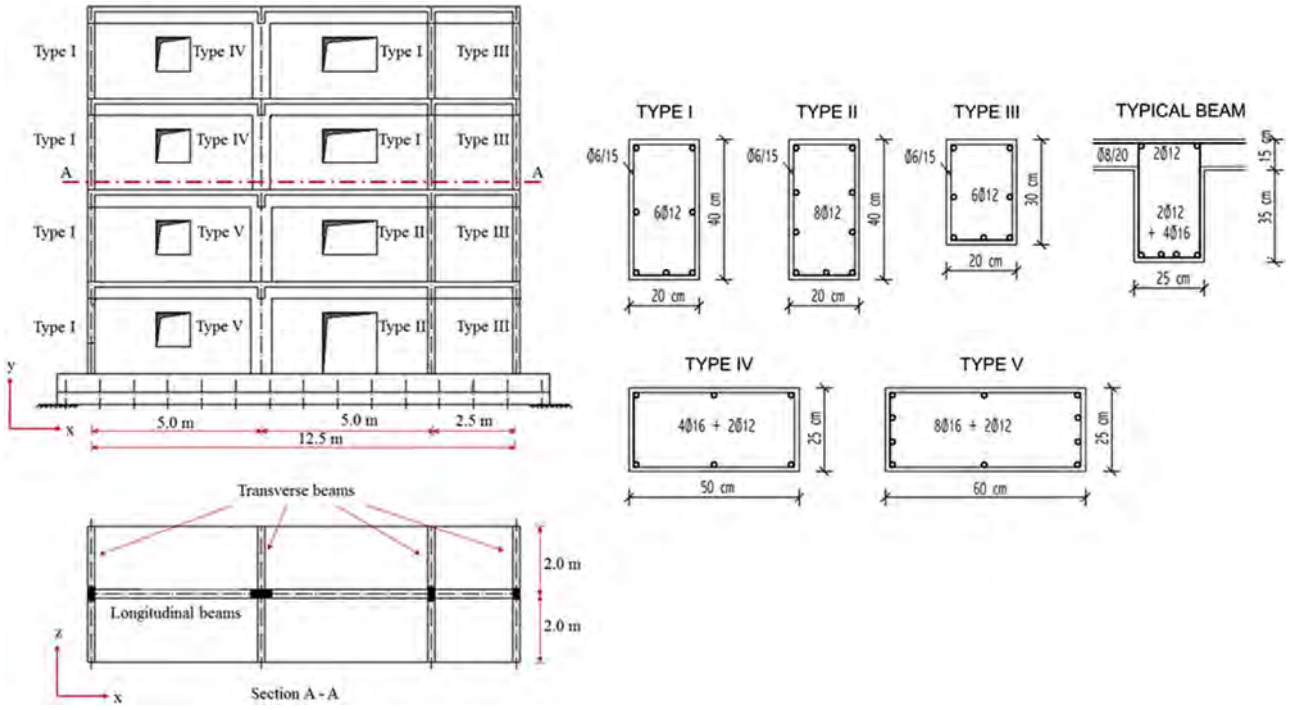

Fig. 5. Plan layout and reinforcement detailing of ICONS frame.

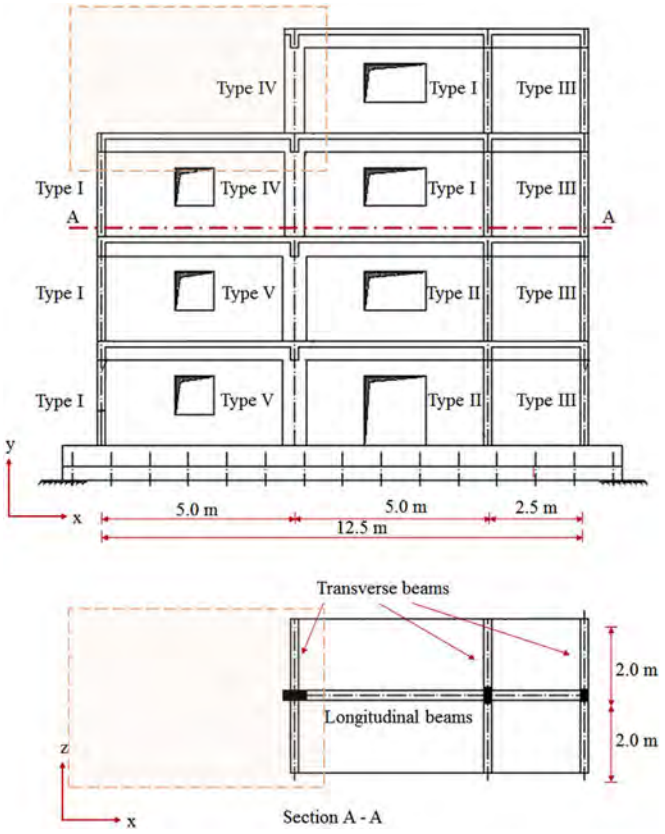

Fig. 6. Introduction of setbacks into ICONS frame.

The structure is then remodeled as an irregular case by altering the place of the structural column elements marked with dashed lines in Fig. 8. Three shear wall elements that were previously located along the E-axis are moved to lie along the G-axis. Hence, the eccentricity of the building is increased. For this case, η_{bi} is determined as 1.21.

4. Modeling assumptions and constitutive material models used in analyses

In this study, fiber-based structural analysis tool ZEUS-NL [9], which was developed at the University of Illinois at Urbana Champaign, is selected to set up 3-D finite element models. To model the structural elements, 3-D cubic elastoplastic beam–column elements are selected. The software is capable of conducting static and dynamic analyses incorporating material and geometric nonlinearity. A mesh of four elements is used for each beam/column member. To accurately capture the high inelasticity induced near the beam-column joints, smaller element sizes are used at the start and end points of each member. The lengths of the elements are 0.15 L and 0.35 L for the outer and inner segments of the beam/column member, respectively, where L is the length of the beam/column member. The element sizes used in this study were determined based on rigorous mesh sensitivity analysis of the frame subjected to constant gravity loads and monotonically increasing lateral loads. The 3-D finite element models of the selected buildings, which were described in previous section, are shown in Fig. 9. Diagonal elements with quite thin and wide cross sections are defined at the floor level to simulate diaphragm behavior. Because the vertical stiffness is ineffective on the diaphragm thickness, horizontal stiffness is taken into account. Rigid diagonal elements are also used to model the bottom story walls.

4.1. Constitutive material models

The classification of non-degrading and degrading systems relies on the material models utilized in the design and assessment of RC structures. Non-degrading material models correspond to conventional concrete and steel models such as the Mander model for concrete [32] and bilinear stress–strain relationships for steel. Because these

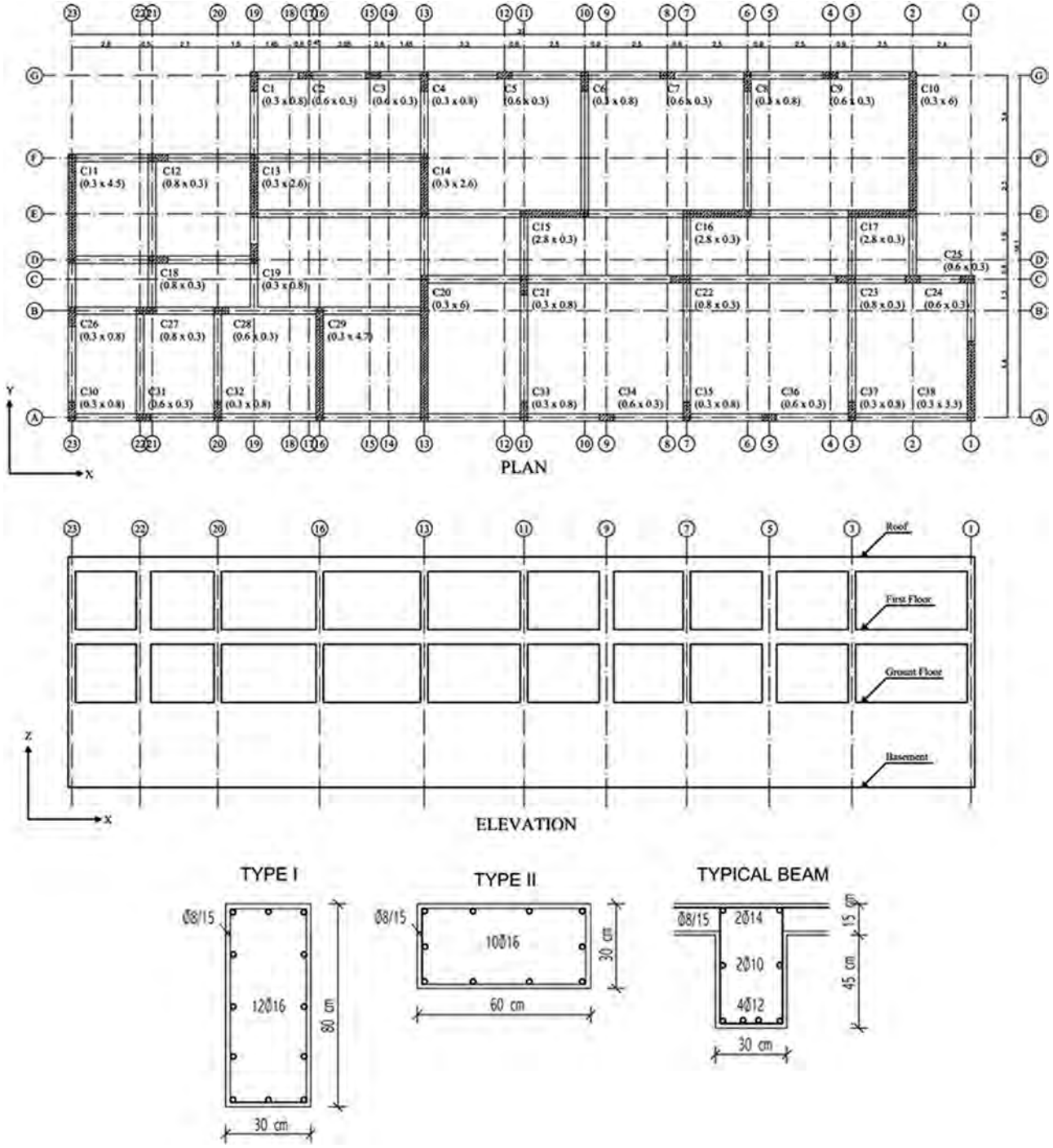

Fig. 7. Plan layout and reinforcement detailing of the considered RC school building.

conventional concrete and steel material models do not consider the stiffness and strength degradation effects under multiple excitations, the plastic-damage model for concrete developed by Lee and Fenves [6] and the modified Menegotto–Pinto steel models [7,8] were implemented in ZEUS-NL [9] as *con5* and *stl4* by Abdelnaby and Elnashai [5]. These degrading 3-D models are evaluated in the nonlinear dynamic analyses and utilized in the present study. Fig. 10 shows a representation of the degrading material models that are used.

It should be highlighted that *con5* (Fig. 10(a)) was developed according to the principles of plasticity and continuum mechanics using the concepts of fracture energy based on multiple hardening variables in order to represent tensile and compressive damages independently [6]. A simple and thermodynamically consistent degradation model is used to simulate the effect of damage on elastic stiffness and its recovery during crack opening and closure (i.e., pinching effects). Furthermore, strength deterioration is modeled using the effective stress of cracked concrete to control the yield surface. In addition, Fig. 10(a) reveals the stiffness and strength degradation of the material response under uniaxial cyclic loading. It can be easily be inferred from the figure that the initial stiffness is different from any other stiffness values of the stress-strain curve owing to degradation. Moreover, the stiffness recovery is revealed at the unloading curves where the stress state changes from tension to compression or vice versa. More information can be found in the paper by Lee and Fenves [6].

The stress-strain relationship of *stl4* relies on the modified Menegotto-Pinto steel model proposed by Gomes and Appleton [8]. The

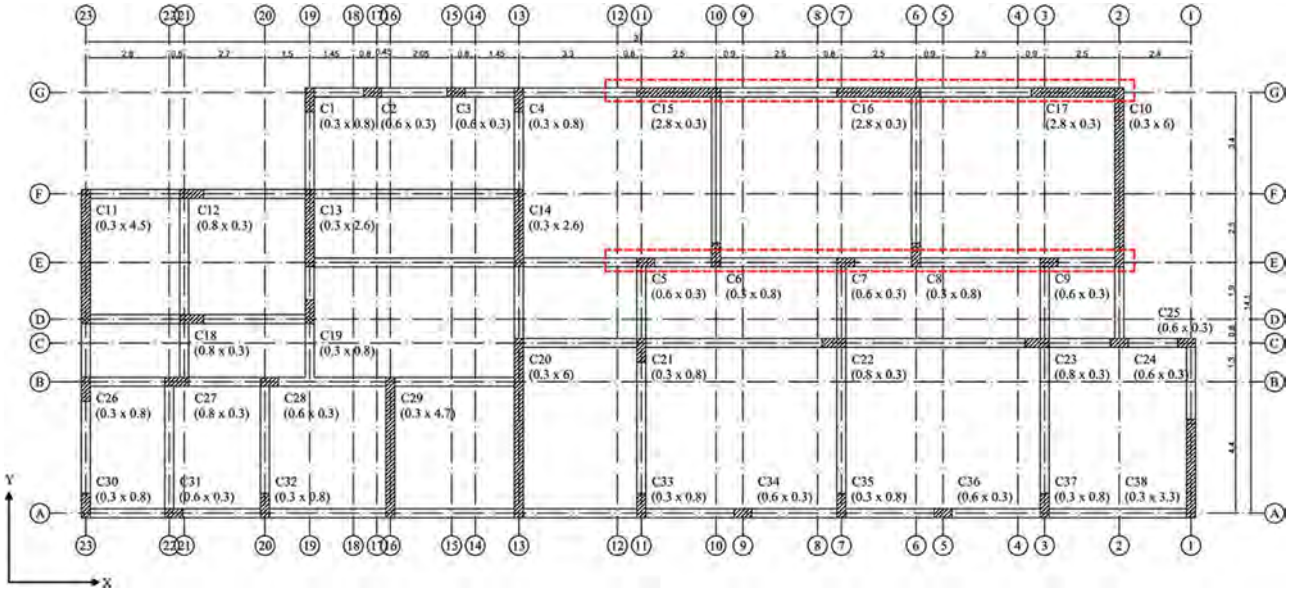

Fig. 8. Alteration of considered RC school building to achieve irregular behavior.

model is capable of simulating the following behaviors:

- elastic yielding and hardening branches in the first cycle,
- Bauschinger effects,
- isotropic strain, which consist of an increase of the envelope curve proportional to the plastic strain component of the previous cycle,
- fracture of reinforcing bars when the fracture strain is exceeded under any cycle,
- inelastic buckling of reinforcing bars after crushing of concrete surrounding bar.

The cyclic behavior is as illustrated in Fig. 10(b) [5]. The reader is referred to Gomes and Appleton [8] for more information regarding the utilized material model.

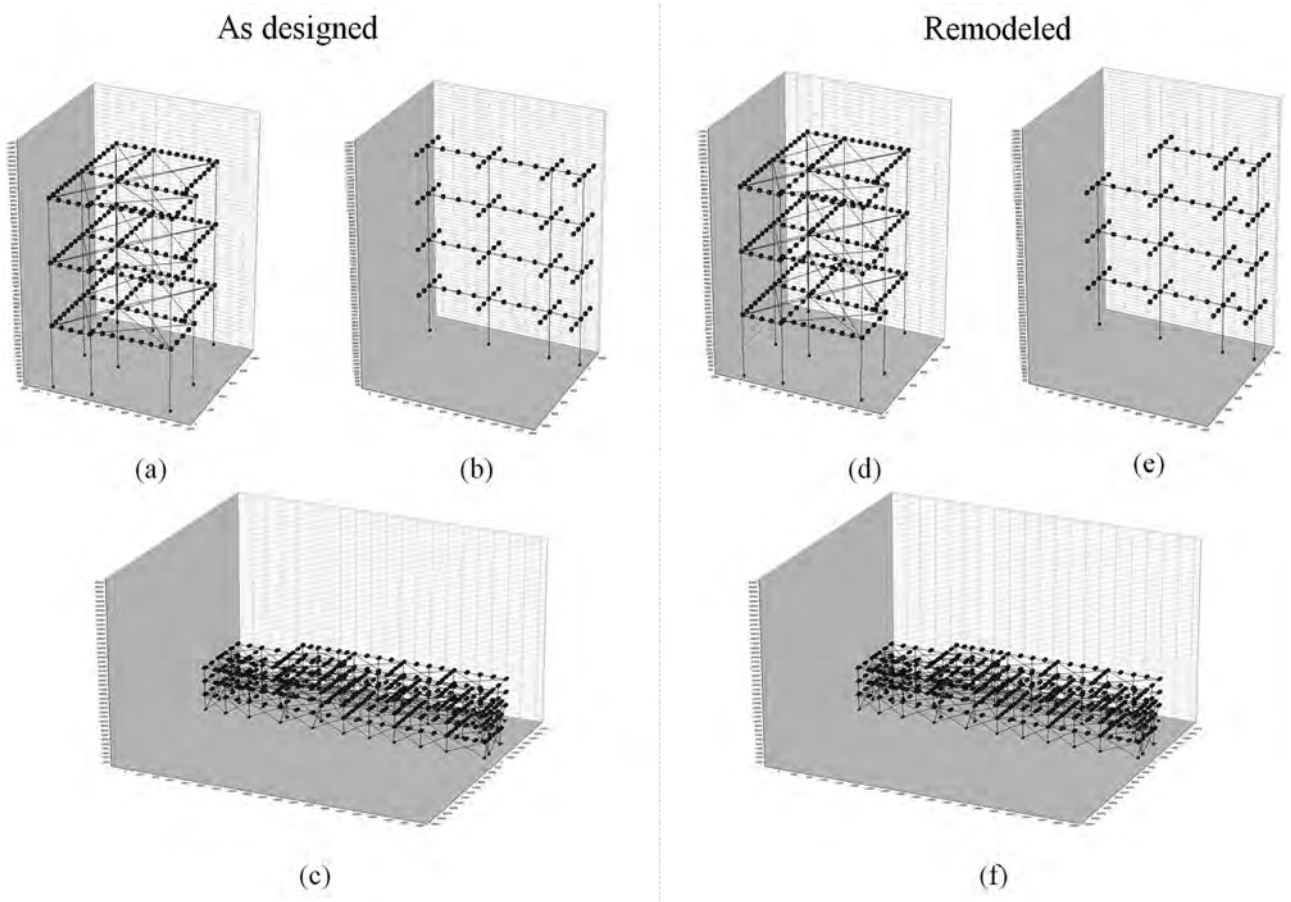

Fig. 9. 3-D finite element models of the selected buildings: (a) and (d) SPEAR frame; (b) and (e) ICONS frame; (c) and (f) school building.

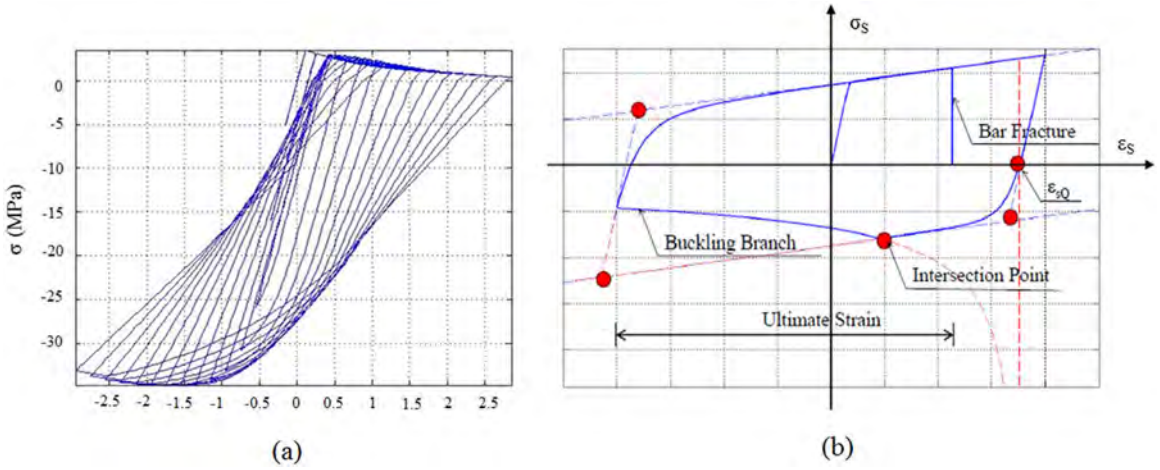

Fig. 10. Material models implemented in ZEUS-NL: (a) degrading concrete model; (b) steel model.

Table 3.
Constitutive material models.

Buildings	Materials						
	stl4					*con5*	
	E (GPa)	σ_y (MPa)	ε_y	ε_u	R_0	f_c (MPa)	E (GPa)
SPEAR	206	400	0.002	0.16	20	25	29
ICONS	200	343	0.001715	0.23	20	16.3	25.5
School Building	200	420	0.0021	0.1	20	30	33

Table 3 contains the constitutive material properties of the considered RC buildings. Regarding the parameters referring to *stl4, E* is the elasticity modulus, σ_y is the yield strength, ε_y is the yield strain, ε_u is the ultimate strain, and R_0 is the constant defined in [8] for taking into account the Bauschinger effect. Further in the cited document, four material constants derived from experiments (i.e. a_1, a_2, a_3, and a_4) are mentioned. These values are assumed to be identical for all the considered buildings. In contrast, regarding the parameters of *con5*, f_c is the compressive strength and E is the elasticity modulus.

4.2. Fiber analysis

Fiber-based finite element modeling is an efficient and accurate tool for simulating the response of a complete structural system under static and dynamic loading conditions. Members of the frame are modeled using elastoplastic beam-column elements, with 200 monitoring points. These elements follow the Euler-Bernoulli formulation [33]. Evaluation of the stiffness matrix of the element is performed at two Gaussian points located at distances approximately 0.3 L from the mid-point of the member. The section at each integration point is further divided into fibers that form the basis of the distributed inelasticity models. Section stiffness is evaluated at the Gaussian points based on the contribution of each fiber. Integration of the stiffness at the Gaussian points yields the tangent stiffness matrix for the element. The element stiffness matrices are assembled into the global stiffness matrix of the whole structure.

4.3. Plastic hinges

A plastic hinge is assumed to form when the strains of the reinforcing bars exceed the yield strain of steel at the sections located at a distance d/2 from the perpendicular element centreline, where d is the depth of the perpendicular element, as shown in Fig. 11.

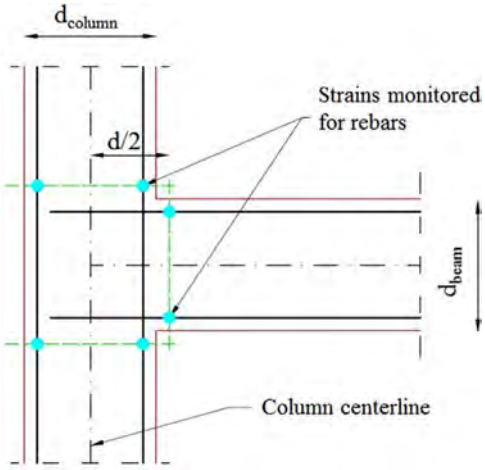

Fig. 11. Beam–column joint showing where strains are monitored in reinforcing bars (marked in blue).

5. Analytical study and results

5.1. Eigenvalue analysis and fundamental periods

To determine the fundamental periods and vibration modes of the considered structures, eigenvalue analyses are performed for both the as designed and modified cases. Lumped masses are assigned at the nodes of beam elements. Mass values are determined by considering both the dead load (D) and live load (Q). Live loads are reduced by a live load reduction factor (n), which changes according to the structure type. For the SPEAR and ICONS buildings, this reduction factor is taken as 0.3, whereas for the school building, it is assumed as 0.6 according to

Table 4
Periods and participation ratios of the considered buildings.

Case	Building	T_1 (s)	U_x (%)	U_y (%)	T_2 (s)	U_x (%)	U_y (%)	T_3 (s)	U_x (%)	U_y (%)
As designed	SPEAR	0.66	70	5	0.61	16	44	0.5	2	34
	ICONS	0.6	84	0	0.21	11	0	0.15	2	0
	School building	0.18	55	0	0.12	0	68	0.09	0	0
Modified	SPEAR	0.64	88	0	0.52	0	85	0.46	0	0
	ICONS	0.62	85	0	0.21	10	0	0.15	2	0
	School building	0.19	51	0	0.13	0	0.67	0.1	3	0

Table 5
Torsional-to-lateral frequency ratios.

Case	Building	ω_x (Hz)	ω_{hx} (Hz)	Ω_x	ω_y (Hz)	ω_{hy} (Hz)	Ω_y
As designed	SPEAR	1.515	1.639	1.08	2	1.639	0.82
	School building	5.555	11.1	2	8.333	11.1	1.33
Modified	SPEAR	1.563	2.174	1.39	1.923	2.174	1.130
	School building	5.263	7.692	1.46	7.692	7.692	1

TEC [31]. The first three natural periods of the considered structures are listed in Table 4. Here, U_x and U_y refer to the modal mass participation ratios in the X- and Y- directions, respectively.

It is a well-known fact that the torsional response of structures depends on many elastic and inelastic parameters. A key elastic parameter is the ratio of the uncoupled torsional frequency ω_θ to the uncoupled lateral frequency ω_h. According to Fajfar et al. [34], this ratio, Ω, has an influence on the torsional behavior of a structure. If Ω is greater than 1, the response is mainly translational and the structure is defined as torsionally stiff; conversely, if Ω is lower than 1, the response is strongly affected by the torsional behavior, and the structure is defined as torsionally flexible [35]. The same reference highlighted that torsionally stiff structures show simpler seismic behavior than torsionally flexible ones. Bhatt and Bento [36] mentioned that a structure can be torsionally stiff in one direction and torsionally flexible in the other. Table 5 contains the torsional-to-lateral frequency ratios for both the as designed and modified cases.

It can be concluded that the SPEAR building is classified as torsionally stiff in the X- direction and torsionally flexible in the Y- direction. After altering the structural geometry, the mentioned frequency ratio is determined to be greater than 1 for both directions, revealing the fact that the structure is now torsionally stiff. Owing to the behavior of the ICONS frame, it was not possible to determine the Ω ratios for this structure. The Ω ratios referring to the damaged RC school building also prove that for the as designed case, the structure is torsionally stiff.

5.2. Capacity assessment of selected structures for as designed and modified cases

In the last decade, there has been a keen interest in nonlinear static procedures (NSPs) and their applications because they require less computational effort than nonlinear dynamic analyses. However, a consensus has not yet been reached on the applicability of NSPs. A recent study conducted by the National Institute of Standards and Technology [37] concluded that for regular and low-rise structures, the N2 procedure, first proposed by Fajfar and Gaspersic [38] and later implemented in EC8 [18], gives good correlation with the nonlinear dynamic analysis results [28]. Therefore, in the present study, the capacities of the regular structures are assessed using the N2 method. Because irregularities arise in the structure when using the N2 method, an extended N2 procedure [39] that considers multimodal effects is applied to derive the pushover curves. Prior to the pushover analyses, the structures are subjected to gravity loads i.e., combinations of $G+nQ$. For the irregular cases, the correction factor for the plan layout for SPEAR is found to be 1.23, and the elevation correction factor for ICONS is found to be 1.02. Though the school building has irregularities in its elevation and plan, the shear walls surrounding the bottom floor reduce the elevation correction factor. The calculated correction factors for the plan and elevation of the school building are determined as 1.12 and 1.01, respectively.

Fig. 12 shows the derived capacity curves obtained by applying the extended N2 method. The graphs reveal that the capacity of the school building is much more than that of the others because of the stiff shear walls at its bottom. The SPEAR and school buildings have higher capacities in the positive direction, whereas the ICONS frame has a higher capacity in the negative direction.

The calculated plastic hinge numbers after applying the aforementioned methodology are presented in Table 6. It should be noted that the difference in the hinge distribution is due to the applied modification method used to change the structures from as designed to

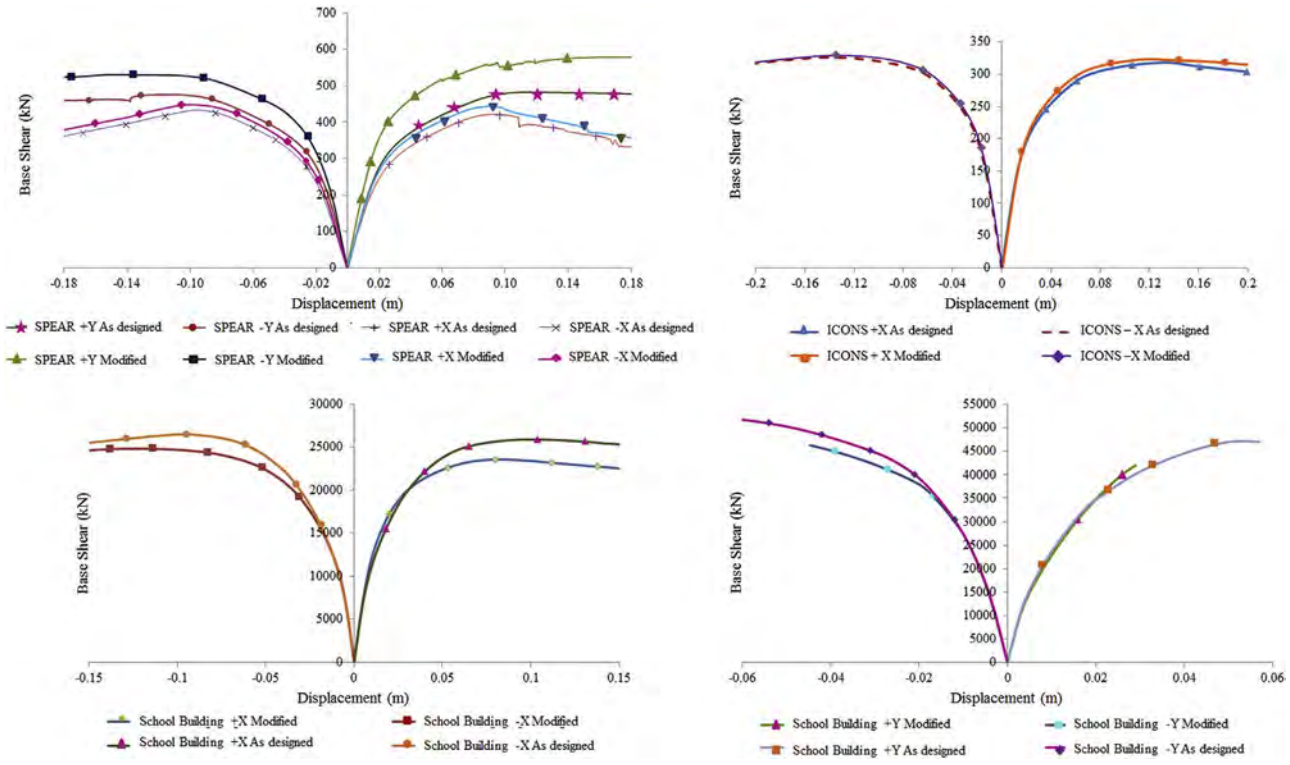

Fig. 12. Capacity curves derived using the extended N2 method.

Table 6
Number of developed plastic hinges.

Case	As designed				Modified			
Direction	+X	-X	+Y	-Y	+X	-X	+Y	-Y
SPEAR	20	28	33	34	22	30	14	25
ICONS	12	12	–	–	11	7	–	–
School building	29	34	0	4	41	32	0	4

modified.

5.3. Irregularity effects on seismic response of degrading models

To consider the irregularity effects on degrading models, nonlinear time history analyses are performed on the case-study RC buildings. The structures are subjected to the mainshock and aftershock sequences of the 2011 Tohoku earthquake recorded from 23 stations (Fig. 1), and 516 total analyses are performed. The previously explained degrading models have been used to determine the residual displacements of the considered buildings under the applied multiple excitations, as shown in Figs. 13, 14, and 15 for both the regular and irregular cases. The seismic responses of the mainshock and aftershocks are shown separately in the illustration to emphasize the damage values. Five records that are evaluated to obtain the maximum differences in the residual displacement values are marked on the graphs. It should be noted that in three of five sequences, some aftershocks have higher PGA values than the mainshock, and the rest have similar PGA values.

Considering the aforementioned five records, the derived top displacement-time traces are plotted in Figs. 16, 17, and 18 for the SPEAR, ICONS, and school buildings, respectively. It is worth mentioning that the residual displacements increase after sequences hit the structures. As can be inferred from Fig. 16, for the regular case of SPEAR frame, no residual displacement is observed after the mainshock; however, a 22-mm displacement occurs after the aftershocks. In contrast, for the irregular case, 42-mm and 31-mm residual displacements are observed after the mainshock and aftershocks, respectively. At the end of all the sequences, the total residual displacement values are 22 mm and 73 mm for the regular and irregular cases, respectively.

For the considered the ICONS frames, a 52-mm residual displacement occurs after the mainshock. Subsequently, the aftershocks alter this by another 35 mm. However, for the irregular case of considered building, these numbers are 102 mm and 94 mm for the mainshock and aftershock, respectively. The total residual values are 87 mm and 196 mm for the regular and irregular cases, respectively. The situation is similar to the SPEAR frame: the aftershocks sequences cause additional displacement and the final displacement is greater in the irregular cases.

As expected, the displacements of the considered RC school building are lower than those of the others, owing the high stiffness of the building. While a 1.3-mm displacement value was observed after the mainshock for the regular case, a 2.3-mm displacement was caused by the aftershocks in the irregular case. Hence, the residual displacement for the irregular case of the considered school building was also greater than its regular counterpart.

The mean drift profiles of the considered structures for the degrading models are presented in Fig. 19. The stories having the maximum drift values are circled on the given graphs. Furthermore, a comparison is carried out in terms of the drift results from the dynamic and nonlinear static pushover procedures in Table 7. The calculated drift values obtained from the N2 and extended N2 methods for the regular and irregular cases of the degrading models are shown in the same figure. It is concluded that the nonlinear static results are in good correlation with the implemented time-history analysis results, especially for the lower stories. For the higher stories, the difference in the results can be attributed to the higher mode effects. Additionally, the drift results for the irregular cases are found to be greater than those for the regular cases.

Because interstory drifts are used as an effective damage control measure in the literature, interstory drift values of the above-assessed story levels are presented in Figs. 20, 21, and 22 considering both the regular and irregular cases of the investigated structures. A code threshold limit of 0.5%, corresponding to the damage state [18], is also plotted on the graphs for comparison.

Inferring from the given plots, the aftershock sequences alter the residual displacement values. The increases in the residual displacement values for the irregular cases are greater than that for their regular counterparts. Furthermore, the code threshold limit is exceeded for both the regular and irregular cases of the SPEAR and ICONS buildings. In contrast, the school building does not breach this limit because of the shear walls surrounding the bottom story.

The base shear–time history traces of the analyzed buildings are plotted in Figs. 23, 24, and 25 for the previously considered earthquake records. The capacity results calculated using the aforementioned NSPs are also marked on the given plots for comparison. It is concluded that the capacities are exceeded for the SPEAR and ICONS frames when the structures are subjected to the mentioned earthquakes. However, the capacities are not exceeded for the school building. This can be explained by the excessive shear wall distribution in the school building.

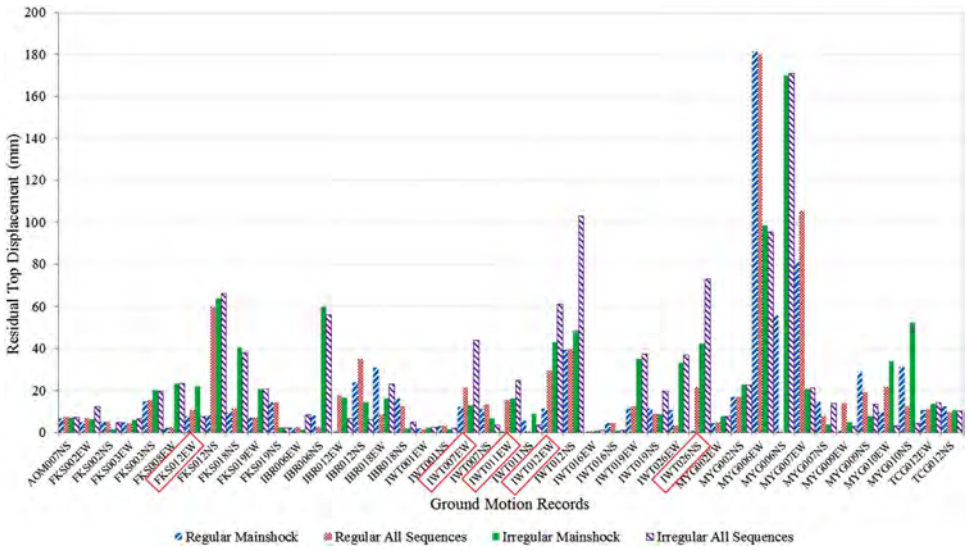

Fig. 13. Residual top displacements for the SPEAR frame under the applied multiple excitations.

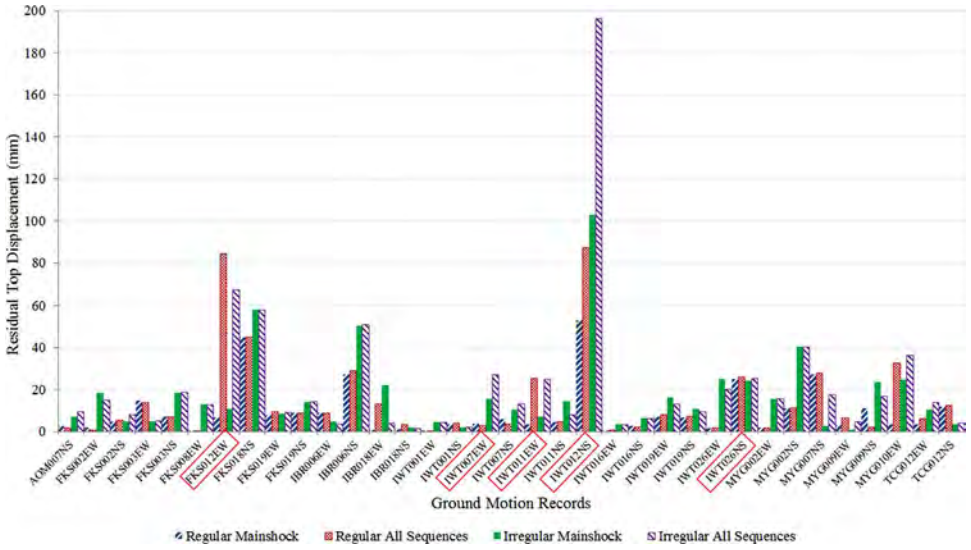

Fig. 14. Residual top displacements for the ICONS frame under the applied multiple excitations.

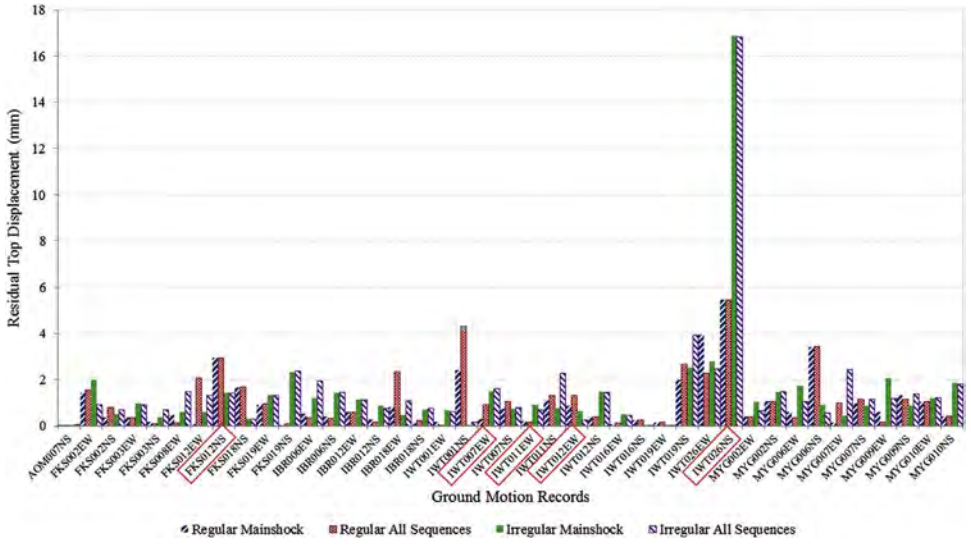

Fig. 15. Residual top displacements for the school building under the applied multiple excitations.

6. Discussion

Many constitutive damage models for RC structures are available, and they have been calibrated in the literature. Namely, Hatzivassiliou and Hatzigeorgiou [40], Zhang et al. [41], and Moshref et al. [42], proposed and validated constitutive damage models for the analysis of concrete structures that are suitable for generic 2- or 3-D applications. Within the framework of continuum damage mechanics, tensile and

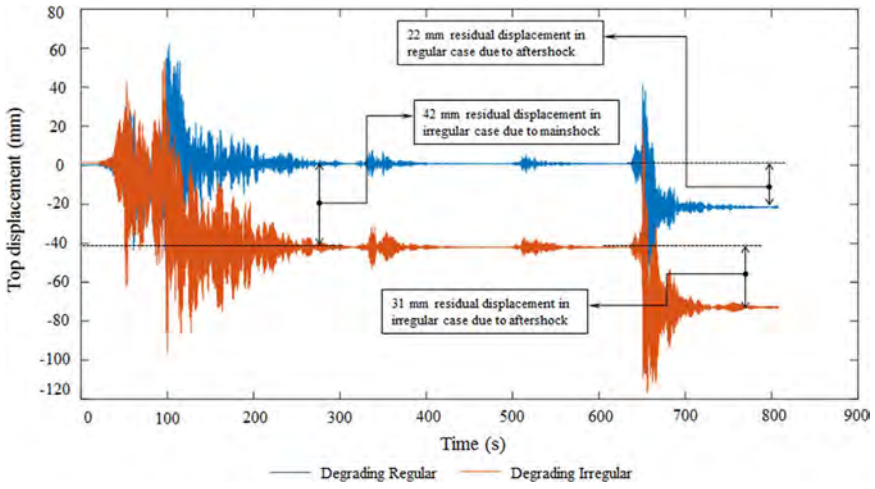

Fig. 16. Displacement sequence of the SPEAR frame under IWT026NS record.

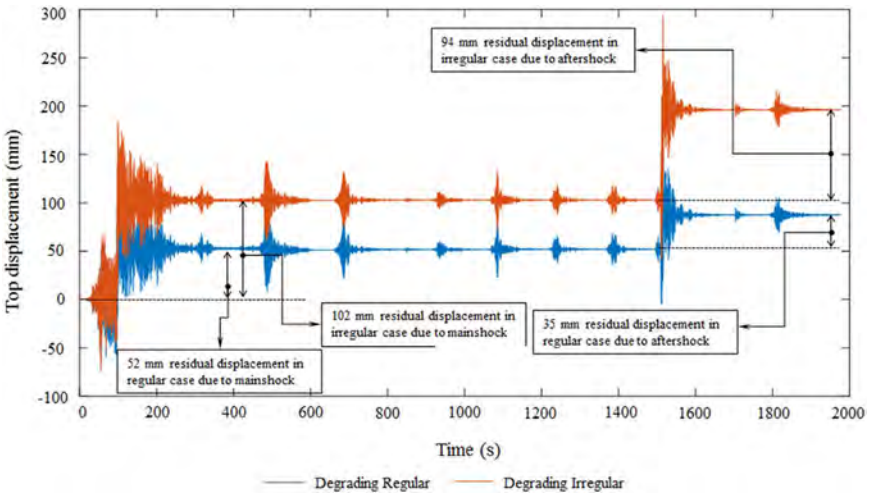

Fig. 17. Displacement sequence of the ICONS frame under IWT012NS record.

shear damage variables are adopted to describe the degradation of the macro-mechanical properties of concrete. Furthermore, Palermo and Trombetti [43] proposed and validated a new modeling strategy for lightly reinforced concrete sandwich panels, incorporating the damage model proposed in the aforementioned studies. These sandwich panels are mainly appealing for developing countries. However, in this study, constitutive damage models, which were previously proposed by Lee and Fenves [6] and Gomes and Appleton [8] and implemented in ZEUS-NL [9] by Abdelnaby and Elnashai [5], are considered for assessing the seismic response of irregular RC structures under multiple excitation sequences.

The seismic responses of the analyzed RC buildings considering both the as designed and modified cases, under the mentioned earthquake excitations are illustrated in Figs. 26, 27, and 28. In Fig. 26, the derived hinge mechanisms obtained after applying the IWT026NS record to the SPEAR frame is presented. The mainshock generates 36 hinges for the considered earthquake; however, the number of calculated hinges increases to 45 when all the sequences are applied to the regular case of the building. For the irregular case under the same conditions 46 and 47 hinges exist after the mainshock and all the sequences, respectively. The formed hinges for the regular and irregular ICON frames under IWT012EW record are presented in Fig. 27. For the regular case, 28 and 31 hinges exist after the mainshock and all the sequences, respectively. For the irregular case, the mainshock generates 32 hinges, but no additional hinges are generated by any of the aftershocks. In Fig. 28, the locations of the derived hinges are shown for the RC school building for the IWT012EW earthquake record. For the regular case, 19 and 32 hinges exist after the mainshock and all the sequences, respectively. These numbers are 11 and 24 for the irregular case under the same excitations.

Formation of hinges after applying the N2 and extended N2 procedures are as presented in Figs. 29, 30, and 31. The disagreement between the results from the dynamic and static analyses in terms of plastic hinges formation is due to the use of EC8 [18] spectrum while on the other hand specific ground motion sequences that do not match EC8 [18] spectrum was used in the dynamic analyses. Reader is referred to Koren and Kilar [44], and Magliulo et al. [45] for more details related with the applicability of N2 procedures.

The average hinge distributions after applying all the recorded strong ground motions, taking into account both the as designed and modified cases, are presented in Fig. 32. The percentage of plastic hinges is normalized according to the results of the regular mainshock values to obtain comparable distribution. For all the considered buildings, the all-sequence excitations gave higher results than the mainshock excitations. Furthermore, it can be concluded that irregularity effects alter the number of formed hinges for both the mainshock and all sequences excitations.

Fig. 33 summarizes the relative residual displacements in terms of the mainshock and aftershocks, considering both the regular and irregular cases for the SPEAR, ICONS, and RC school buildings. When comparing the main shocks for the SPEAR, ICONS, and RC school buildings under the given excitations, the residual displacements of the irregular cases are approximately 27%, 35%, and 29%, respectively, higher than those of the regular cases. In addition, for the SPEAR,

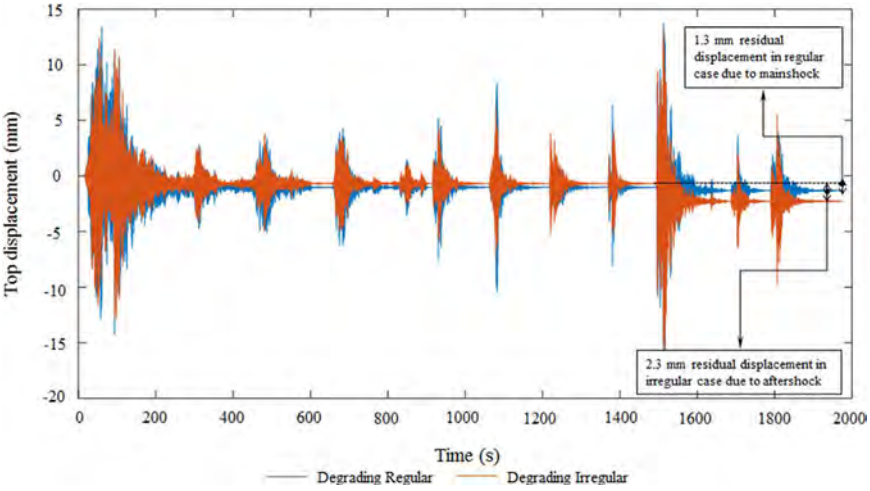

Fig. 18. Displacement sequence of the school building under IWT012EW record.

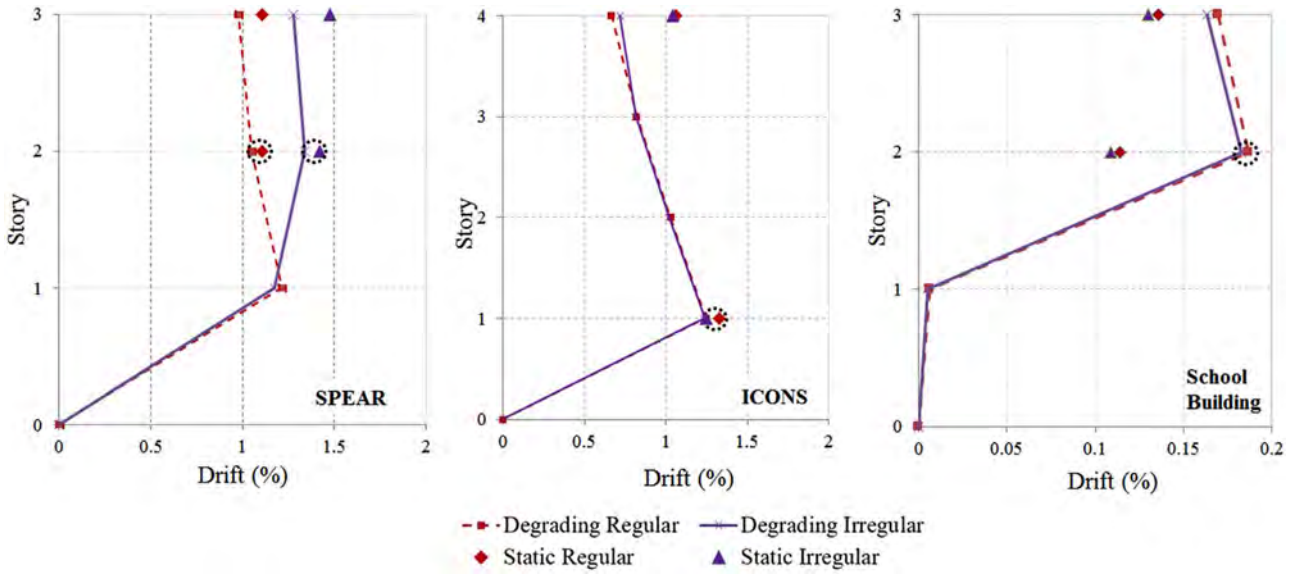

Fig. 19. Mean drift profiles of the considered structures.

Table 7
Comparison of nonlinear dynamic and static analysis results in terms of drift values.

Building	SPEAR				ICONS				School Building			
Analysis Type	Dynamic		Static		Dynamic		Static		Dynamic		Static	
Case	1*	2*	1	2	1	2	1	2	1	2	1	2
Story 1	1.172	1.215	1.084	1.088	1.245	1.236	1.33	1.25	0.006	0.005	0.005	0.003
Story 2	1.337	1.05	1.42	1.092	1.027	1.018	1.266	1.246	0.186	0.182	0.112	0.107
Story 3	1.278	0.978	1.476	1.033	0.82	0.814	1.219	1.123	0.169	0.162	0.142	0.135
Story 4	–	–	–	–	0.665	0.718	1.064	1.04	–	–	–	–

1* As designed.
2* Modified.

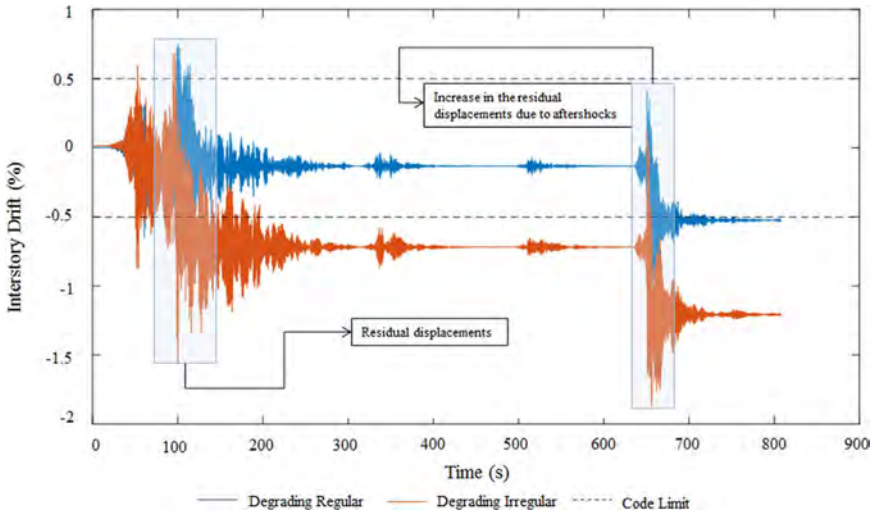

Fig. 20. Interstory drift sequence of the SPEAR frame under IWT026NS record.

ICONS, and RC school buildings, the residual displacements for the irregular cases after all sequences are 28%, 36%, and 35%, respectively, higher than those of the regular cases. Furthermore, for the SPEAR, ICONS, and RC school buildings, it should be noted that considering the aftershock sequences increases the residual displacements by 6%, 22%, and 3%, respectively, for the regular cases and by 7%, 23%, and 9%, respectively, for the irregular cases.

These results clearly show an increase in the residual displacements after the aftershock sequences and the effect of irregularities under multiple earthquake excitations. However, in rare cases, the characteristics of the aftershocks cause them to not increase the residual displacements. In addition, eight of the analyses were not completed because of convergence problems caused by excessive displacements. Moreover, the inability to accurately predict the response of structures under multiple sequences using non-degrading models has been demonstrated in this study.

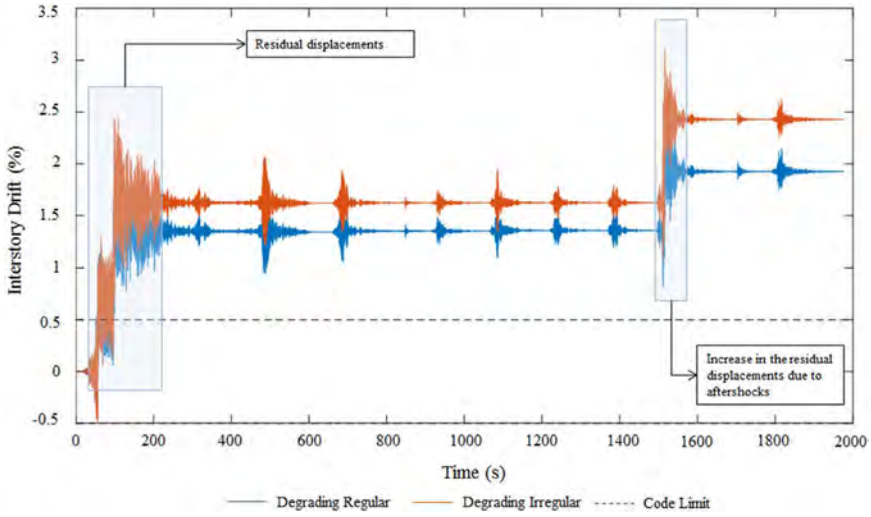

Fig. 21. Interstory drift sequence of the ICONS frame under IWT012NS record.

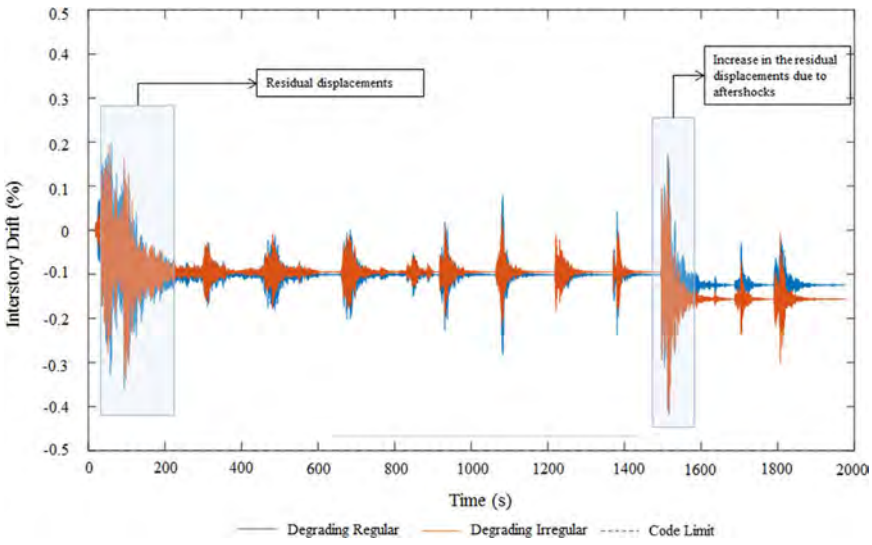

Fig. 22. Interstory drift sequence of the school building under IWT012EW record.

7. Summary and conclusion

In this study, three types of buildings, namely, SPEAR, ICONS, and an as-built school building in Turkey, were investigated under the main shock and aftershocks of as-recorded ground motion sequences obtained from the M_w 9.0 March 11, 2011 Tohoku earthquake. Each building is characterized by high structural irregularity in plan or elevation. Numerical fiber-based finite element models of these buildings, as opposed to idealized system-level and component-level models used in the literature to study multiple earthquake effects, were established using ZEUS-NL [9] analysis tool. The models contained appropriate damage features that are capable of depicting the damage accumulation

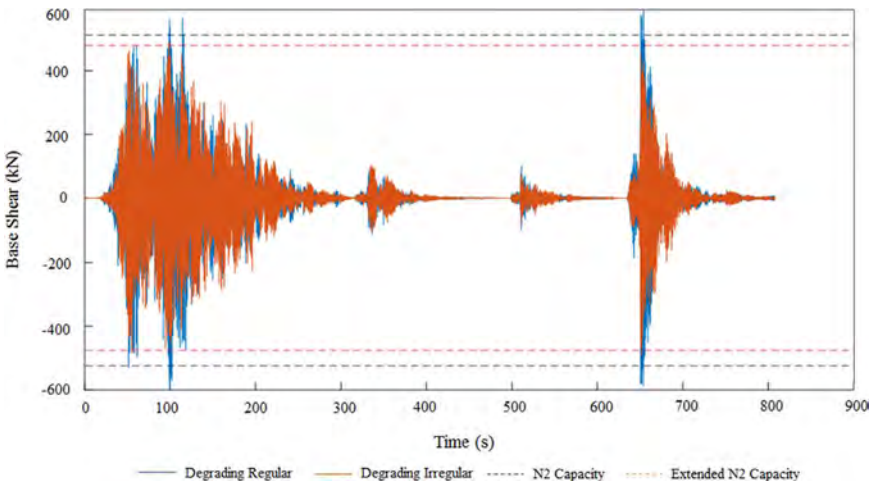

Fig. 23. Base shear-time trace of the SPEAR frame under IWT026NS record.

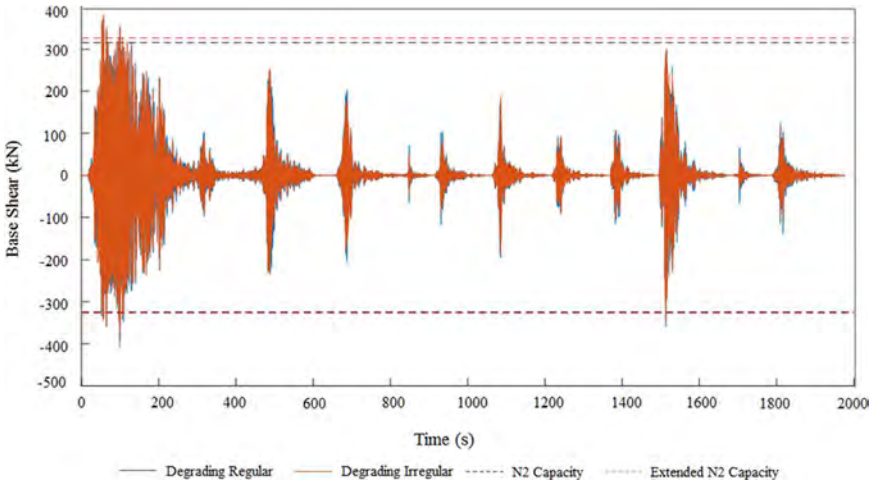

Fig. 24. Base shear-time trace of the ICONS frame under IWT012NS record.

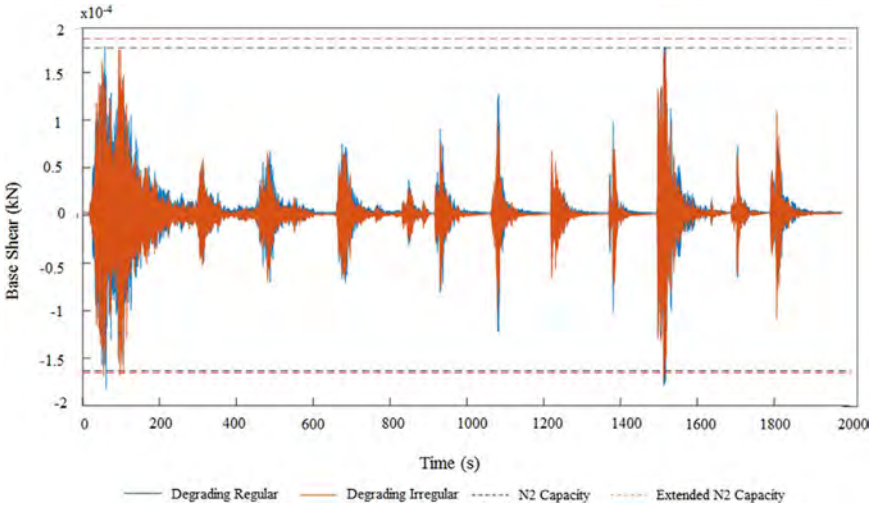

Fig. 25. Base shear-time trace of the school building under IWT012EW record.

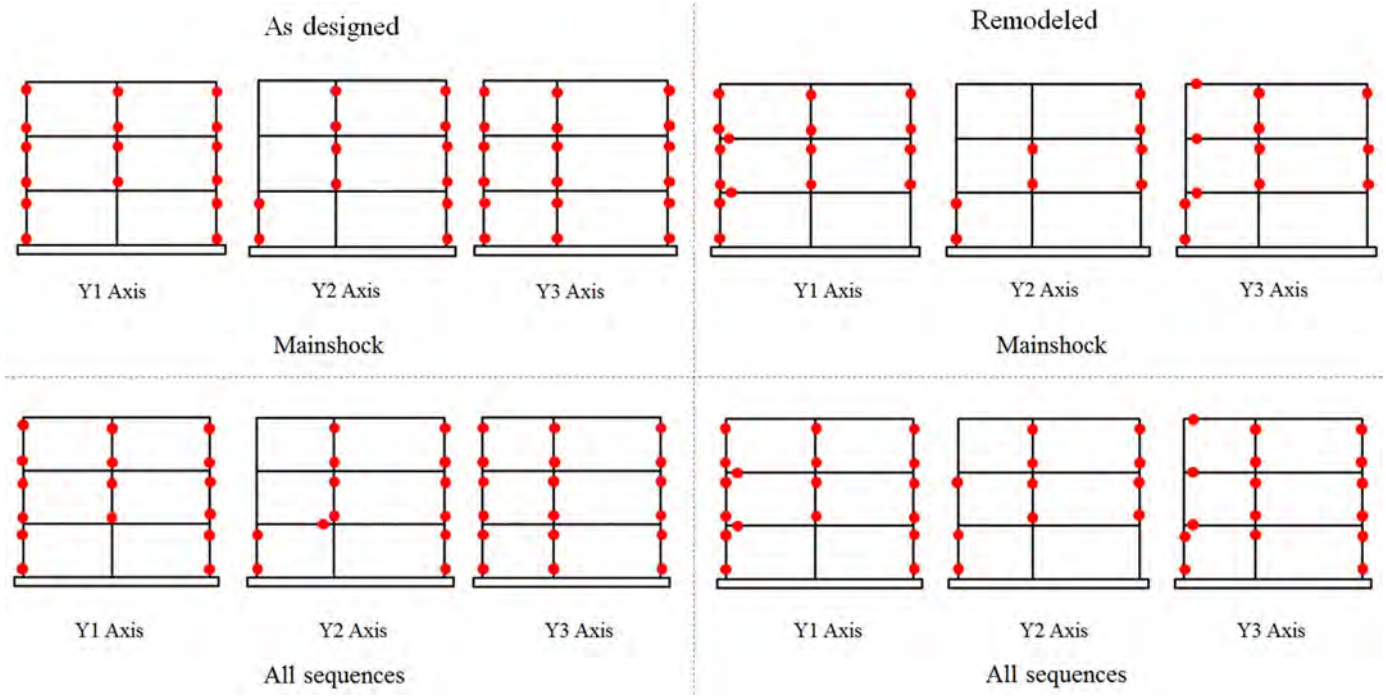

Fig. 26. Hinge mechanisms derived after applying the IWT026NS record to the SPEAR frame.

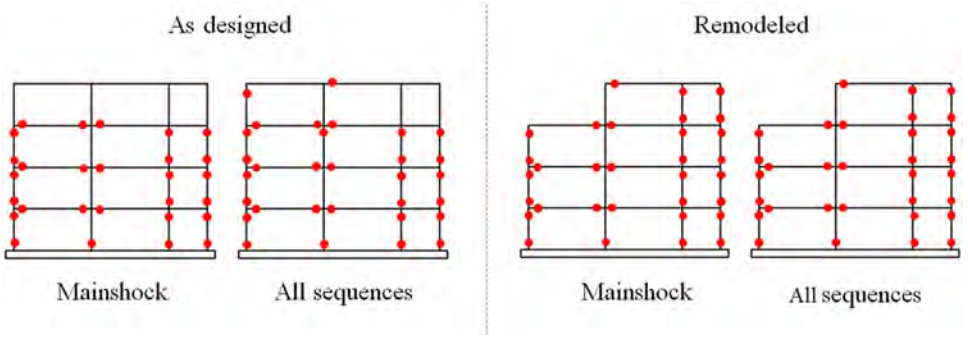

Fig. 27. Hinge mechanisms derived after applying the IWT012NS record to the ICONS frame.

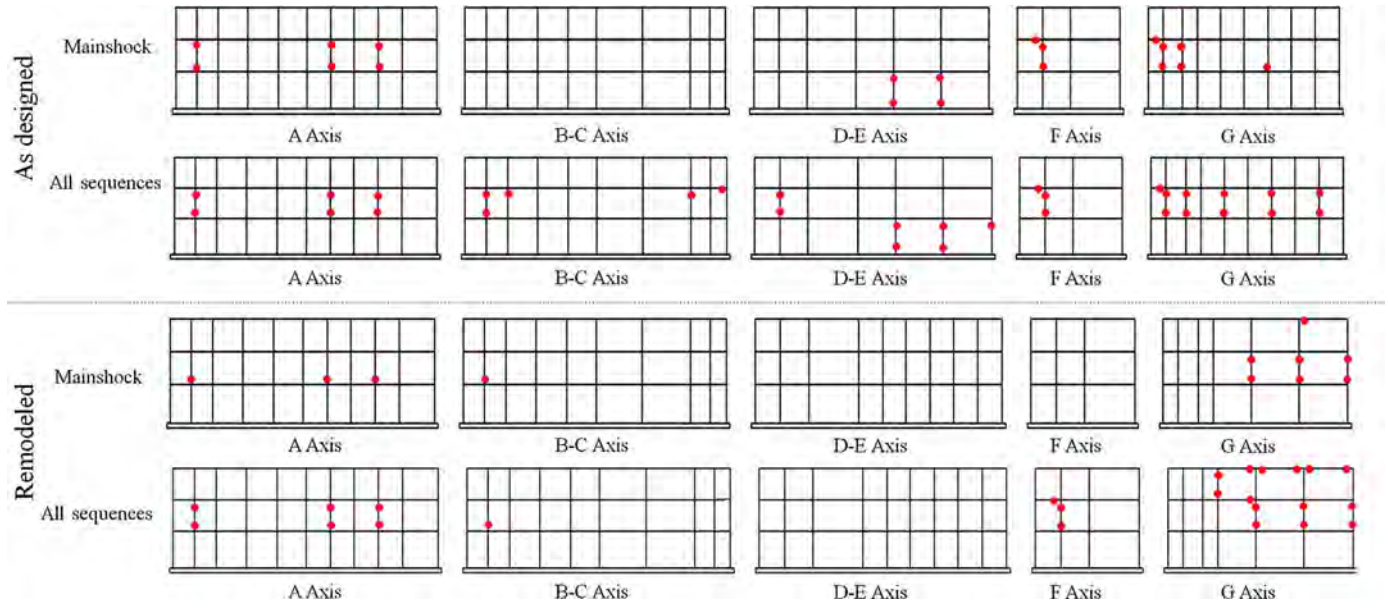

Fig. 28. Hinge mechanisms derived after applying the IWT012EW record to the school building.

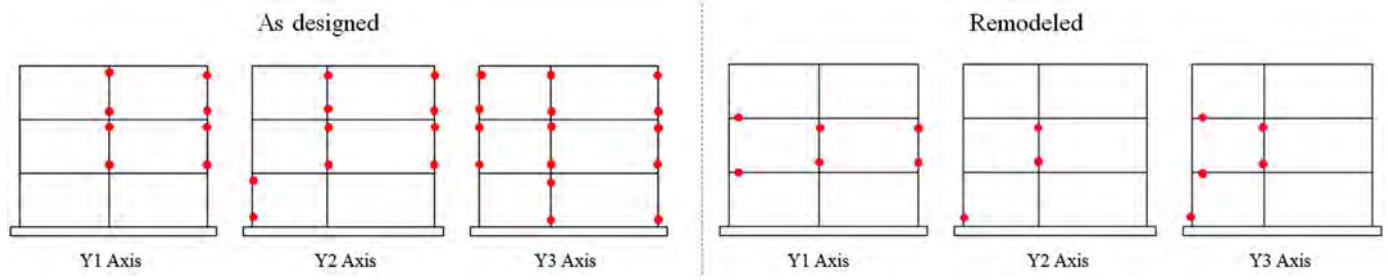

Fig. 29. Hinge mechanisms derived after applying the N2 method to the SPEAR building.

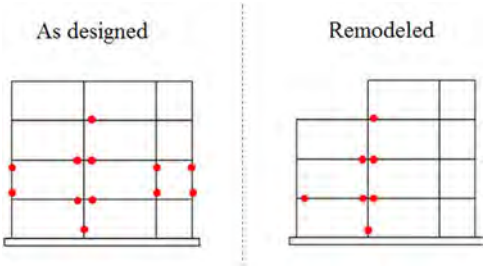

Fig. 30. Hinge mechanisms derived after applying the N2 method to the ICONS building.

effects in terms of stiffness degradation and strength deterioration on the concrete and steel material level as a result of repeated earthquake shocks. The structural characteristics of these buildings were then altered to achieve a regular case while maintaining the same overall stiffness. Numerical models for the regular case were similarly developed, and the capacities of both the regular and irregular structures were evaluated using the N2 and extended N2 procedures. The N2 and extended N2 analyses were also performed for the same buildings but using non-degrading material models for steel (bi-linear) and concrete [32]. The results from the N2 and N2 extended analyses indicated that the non-degrading models cannot accurately capture the damage accumulation effects on the buildings especially when subjected to more than one earthquake. Therefore, the degrading models were only used for the inelastic nonlinear response history analyses, where the three structures were subjected to a suite of ground motion sequences measured at 23 selected stations. The selected ground motion sequences contained a wide variation of ground motion parameters with no consideration given to near-fault effects. The responses of the regular and

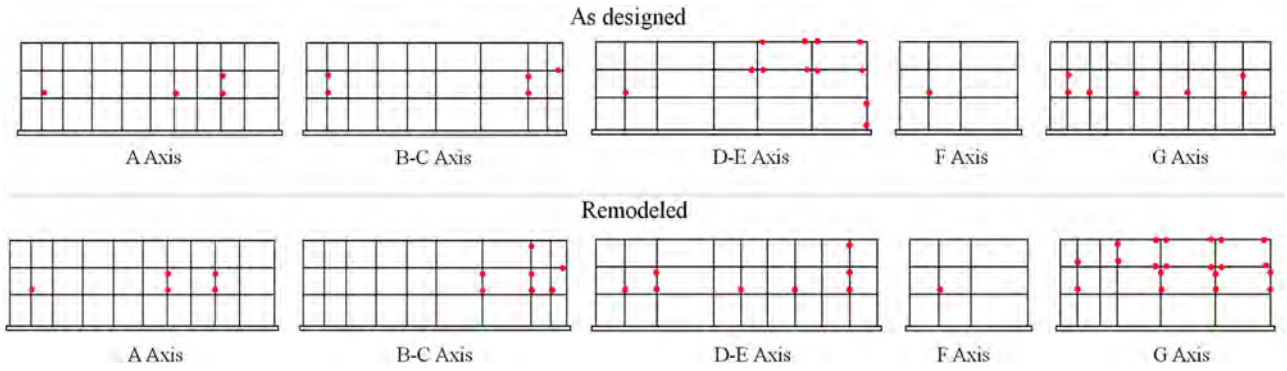

Fig. 31. Hinge mechanisms derived after applying the N2 method to the school building.

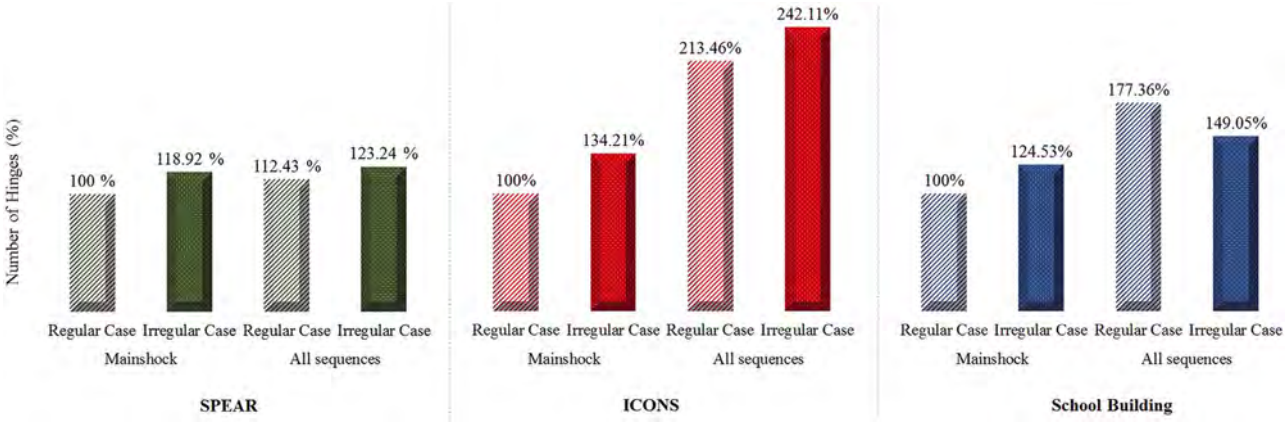

Fig. 32. Average hinge distributions for all considered building–shock–case combinations.

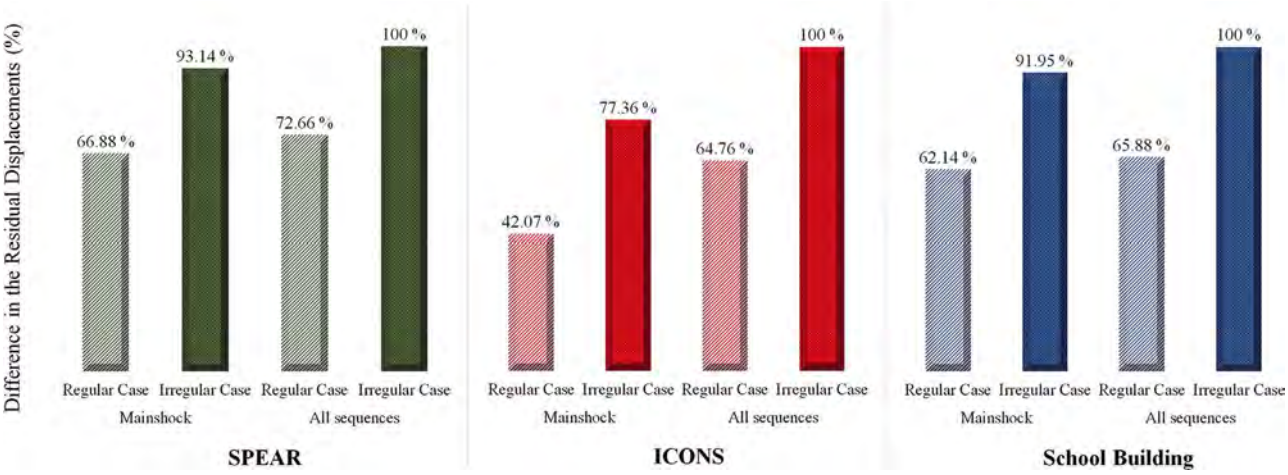

Fig. 33. Relative residual displacements for all considered building–shock–case combinations.

irregular structures were compared, and the following conclusions were drawn:

1. Earthquake sequences impose higher displacement demands on irregular structures compared to their regular counterparts. The average increase in the residual drifts due to structural irregularity is 27%, 35%, and 34% for the SPEAR, ICON, and school buildings, respectively when subjected to the Tohoku earthquake ground motion sequences.
2. Damage accumulation effects from the main shock are of higher significance for irregular structures compared to the regular case because the average percentage increase in the total number of plastic hinges due to aftershocks is 12% and 113% for the regular and 23% and 142% for the irregular SPEAR and ICON buildings, respectively.
3. Multiple earthquake effects cannot be accurately captured using simple numerical analysis methods (commonly used for seismic assessment of structures) where the numerical models do not contain appropriate features that account for accumulation of damage in structural materials and components as a result of repeated earthquake shaking. Hence, for studying the response of structures subjected to multiple earthquakes, models with appropriate damage features have to be employed.
4. N2 and extended N2 methods are effective methods to determine the capacity for irregular structures subjected to multiple earthquakes because their response agreed well with the results obtained from

dynamic response history analyses. However, some discrepancies were observed owing to the effects of higher modes that are not captured by these methods.

5. This research focuses on the seismic response of three buildings only subjected to multiple earthquakes from the Tohoku earthquake sequence. Therefore, the results from this study are limited to this case. However, the outcomes highlight the need for conducting a more detailed analysis to formulate robust design procedures for systems prone to multiple earthquakes with short time span between individual earthquakes in the sequence.

Acknowledgement

This research has been funded by the Istanbul Technical University under Award Number 38873. This support is gratefully acknowledged. All opinions, findings, conclusions, and recommendations expressed in this material are those of the authors and do not necessarily reflect those of the funding body. The efforts of PhD. Candidate Evrim Oyguc to improve the editorial quality of the paper is highly appreciated.

References

[1] Aschheim M, Black E. Effects of prior earthquake damage on response of simple stiffness-degrading structures. Eng Spectra 1999;15:1–24.
[2] Amadio C, Fragiacomo M, Rajgelj S. The effects of repeated earthquake ground motions on the non-linear response of SDOF systems. Earthq Eng Struct Dyn 2003;32(2):291–308.
[3] Hatzigeorgiou GD, Beskos DE. Inelastic displacement ratios for SDOF structures subjected to repeated earthquakes. Eng Struct 2009;31:2744–55.
[4] Hatzigeorgiou GD, Liolios AA. Nonlinear behavior of RC frames under repeated strong ground motions. Soil Dyn Earthq Eng 2010;30:1010–25.
[5] Abdelnaby AE, Elnashai AS. Performance of degrading reinforced concrete frame systems under the Tohoku and Christchurch earthquake sequences. J Earthq Eng 2014;18(7):1009–36.
[6] Lee J, Fenves G. Plastic damage model for cyclic loading of concrete structures. J Eng Mech 1998;124(8):829–900.
[7] Menegotto M, Pinto P. Method of analysis for cyclically loaded RC plane frames including changes in geometry and non-elastic behavior of elements under combined normal force and bending. In: Symposium Resistance and Ultimate Deformability of Structures Acted on by Well Defined Repeated Loads. IABSE Reports. Vol 13. Lisbon.
[8] Gomes A, Appleton J. Nonlinear cyclic stress-strain relationship of reinforcing bars including buckling. Eng Struct 1997;19(10):822–6.
[9] Elnashai AS, Papanikolaou V, Lee D. ZEUS-NL – A system for inelastic analysis of structures. -Am Earthq Cent Univ Ill Urbana-Champaign Program Release 2002.
[10] Takewaki I, Murakami S, Fujita K, Yoshitomi S, Tsuji M. The 2011 off the pacific coast of Tohoku earthquake and response of high-rise buildings under long period ground motions. Soil Dyn Earthq Eng 2011;31:1511–28.
[11] Japan Meteorological Agency. 〈http://www.jma.go.jp/jma/en/2011_Earthquake/Information_on_2011_Earthquake.html〉. [Accessed 12 November 2015].
[12] Goto H, Morikawa H. Ground motion characteristics during the 2011 off the pacific coast of Tohoku earthquake. Soils Found 2012;52(5):769–79.
[13] Zhao D. The 2011 Tohoku earthquake (Mw 9.0) sequence and subduction dynamics in western pacific and east Asia. J Asian Earth Sci 2015;98:26–49.
[14] Kazama M, Noda T. Damage statistics (summary of the 2011 off the pacific coast of Tohoku earthquake damage). Soils Found 2012;52(5):780–92.
[15] Huang Z, Zhao D. Mechanism of the 2011 Tohoku-oki earthquake (Mw 9.0) and tsunami: insight from seismic tomography. J Asian Earth Sci 2013;70–71:160–8.
[16] National Research Institute for Earth Science and Disaster Prevention. NIED. 〈http://www.kyoshin.bosai.go.jp/〉. [Accessed 12 November 2015].
[17] Federal Emergency Management Agency. Prestandard and commentary for the seismic rehabilitation of buildings. FEMA 356. Washington DC, U.S.A; 2000.
[18]. Comité Europeen de Normalization. Eurocode 8: Design of Structures for Earthquake Resistance - Part 1: General Rules, Seismic Actions and Rules forBuildings. 1998-1: 2005, CEN. Brussels, Belgium; 2006.
[19] Turkish Earthquake Code. TEC. Specification for structures to be built in disaster areas, Ministry of Public Works and Settlement, Ankara, Turkey; 1975.
[20] Fardis MN. Design of an irregular building for the SPEAR project-description of the 3-storey structure. Res Report Univ Patras Greece 2002.
[21] Mola E, Negro P. Full-scale PsD testing of the torsionally unbalanced SPEAR structure in the as built and retrofitted configurations. in: SPEAR Workshop – An event to honour the memory of J Donca, EUR 21768 EN. European Commision. JRC, Ispra, IT:139-154; 2005.
[22] Jeong SHJ, Elnashai AS. Analytical assessment of an irregular RC full scale 3D test structure. -Am Earthq Cent Univ Ill Urbana-Champaign USA 2004.
[23] Papanikolaou VK, Elnashai AS, Pareja JF. Limits of applicability of conventional and adaptive pushover analysis for seismic response assessment. -Am Earthq Cent Univ Ill Urbana-Champaign USA 2005.
[24] Stratan A, Fajfar P. Seismic assessment of the SPEAR test structure. IKPIR report. University of Ljubljana. Czech Repub 2003.
[25] Pinho R, Elnashai AS. Dynamic collapse testing of a full-scale four storey RC frame. ISET. J Earthq Technol 2000;37(4):143–63.
[26] Carvalho EC, Coelho E, Compos-Costa A. Preparation of the full-scale test on reinforced concrete frames: characteristic of the test specimens, materials and testing conditions. ICONS report. innovative seismic design concepts for new and existing structures. European TMR. Netw, LNEC 1999.
[27] Di Sarno L, Yenidogan C, Erdik M. Field evidence and numerical investigation of the Mw = 7.1 October 23 van, Tabanlı and the Mw > 5.7 November earthquakes of 2011. Bull Earthq Eng 2013;11:313–46.
[28] Oyguc R. Seismic performance of RC school buildings after 2011 Van earthquakes. Bull Earthq Eng 2016;14(3):821–47.
[29] Çavdar Ö, Bayraktar A. Nonlinear earthquake performance evaluation of a structure collapsed during the van, Turkey, earthquake on October 23, 2011. J Perform Constr Facil 2016;30(4). [: -1–1].
[30] Oyguc R, Guley E. Performance assessment of aseismically designed RC school buildings after October 23, 2011 Van earthquake. J Perform Constr Facil 2017. http://dx.doi.org/10.1061/(ASCE)CF.1943-5509.0000938.
[31] Turkish Earthquake Code. TEC. Specification for structures to be built in disaster areas. Ministry of Public Works and Settlement, Ankara, Turkey; 2007.
[32] Mander JB, Priestley MJN, Park R. Theoretical stress-strain model for confined concrete. J Struct Eng 1986;114(8):1804–25.
[33] Izzuddin BA, Elnashai AS. Eulerian formulation for large-displacement analysis of space frames. J Eng Mech 1993;119(3):549–69.
[34] Fajfar P, Marusic D, Perus I. Torsional effects in the pushover-based seismic analysis of the buildings. J Earthq Eng 2005;9(6):831–54.
[35] Cosenza E, Manfredi G, Realfonzo R. Torsional effects and regularity conditions in RC buildings. In: Proceedings of the 12th Word Conference On Earthquake Engineering. Auckland, New Zealand; 2000.
[36] Bhatt C, Bento R. Estimating torsional demands in plan irregular buildings using pushover procedures coupled with linear dynamic response spectrum analysis. Geotech, Geol Earthq Eng 2013;24:219–33.
[37] Applied Technology Council. Applicability of nonlinear multiple-degree-of-freedom modeling for design. ATC-76-6. National Institute of Standards and Technology. California, U.S.A; 2010.
[38] Fajfar P, Gaspersic P. The N2 method for the seismic damage analysis of RC buildings. Earthq Eng Struct Dyn 1996;25:31–46.
[39] Kreslin M, Fajfar P. The extended N2 method considering higher mode effects in both plan and elevation. Bull Earthq Eng 2012;10:695–715.
[40] Hatzivassiliou M, Hatzigeorgiou GD. Seismic sequence effects on three-dimensional reinforced concrete buildings. Soil Dyn Earthq Eng 2015;72:77–88.
[41] Zhang S, Wang G, Sa W. Damage evaluation of concrete gravity dams under mainshock-aftershock seismic sequences. Soil Dyn Earthq Eng 2013;50:16–27.
[42] Moshref A, Khanmohammadi M, Tehranizadeh M. Assessment of the seismic capacity of mainshock-damaged reinforced concrete columns. Bull Earthq Eng 2017;15:291–311.
[43] Palermo M, Trombetti T. Experimentally-validated modeling of thin RC sandwich walls subjected to seismic loads. Eng Struct 2016;119:95–109.
[44] Koren D, Kilar V. The applicability of the N2 method to the estimation of torsional effects in asymmetric base-isolated buildings. Earthq Eng Struct Dyn 2011;40:867–86.
[45] Magliulo G, Maddaloni G, Cosenza E. Extension of N2 methods to plan irregular buildings considering accidental eccentricity. Soil Dyn Earthq Eng 2012;43:69–84.